Received: 1 November 2021 | Revised: 18 April 2022 | Accepted: 19 April 2022

DOI: 10.1002/hyp.14584

RESEARCH ARTICLE

WILEY

Event scale hydrograph responses highlight impacts of widespread stream burial and urban infrastructure failures

Rebecca Forgrave | Emily M. Elliott | Daniel J. Bain

Department of Geology and Environmental Science, University of Pittsburgh, Pittsburgh, Pennsylvania, USA

Correspondence
Rebecca Forgrave, SRCC 200, 4107 O'Hara St, Pittsburgh, PA 15260, USA.
Email: ref61@pitt.edu

Funding information
National Science Foundation, Grant/Award Numbers: 1253000, 1939977

Abstract

Fast hydrologic responses to storms in urban areas are often attributed to high percentages of impervious surfaces; however, another factor affecting urban storm response is channel burial. No previous studies have documented storm event responses in buried streams despite how common stream burial is in urban areas, with some US cities having over 75% of all headwater channels buried. Understanding event dynamics is particularly important as climate change predictions suggest an increase in frequency of high intensity storms and urban flooding. This study used 15-min precipitation and discharge data over a period of 6.5 years to categorize storm event responses in Nine Mile Run, an urban watershed in Pittsburgh, Pennsylvania where 98% of all channels are buried. Extensive stream burial led to lower watershed retention capacity and resulted in faster storm event responses relative to other urban streams with comparable imperviousness. Additionally, urban water subsidies in the form of sewer overflows, hydrant flushing, or water line breaks can have measurable contributions to flow event responses and result in seemingly unfeasible runoff ratios. This study demonstrates novel watershed runoff responses in systems dominated by subsurface infrastructure, which play a key role in urban water balance. Additionally, this study highlights the fact that stream restoration is not a universal solution to urban stream flashiness because downstream restoration cannot resolve the impacts of upstream burial.

KEYWORDS
buried streams, hydrograph analysis, infrastructure, rainfall-runoff responses, stormwater, urbanization

1 | INTRODUCTION

The impacts of urbanization on hydrologic response to storms are well-known: urban hydrographs are characterized by a steeper rising limb, higher peak flow, and shorter recession compared to similarly-sized rural watersheds. These impacts on flow scale with increasing watershed imperviousness and percent of landscape served by storm drainage systems. (Leopold, 1968; Schueler, 1994; Schueler et al., 2009; Shuster et al., 2005). However, stream burial, the process of relocating surface water channels into subsurface pipes, is another common characteristic of urban watersheds that has not received as much attention in terms of its effect on runoff routing and storm responses (Graf, 1975). Some buried streams are given their own pipe networks while others are deliberately captured by existing sewers (Broadhead et al., 2013).

A more precise understanding of hydrologic response to precipitation in buried streams on an event-by-event basis is important for storm water management and flood prevention (Merz et al., 2012) both now and into the future. Predicted climactic shifts will impact the hydrologic cycle both globally and locally (Kundzewicz, 2008; Trenberth, 1999) as warmer air can hold more moisture, increasing annual rainfall and the frequency of intense precipitation events

Received: 1 November 2021 | Revised: 18 April 2022 | Accepted: 19 April 2022

DOI: 10.1002/hyp.14584

RESEARCH ARTICLE

WILEY

Event scale hydrograph responses highlight impacts of widespread stream burial and urban infrastructure failures

Rebecca Forgrave | Emily M. Elliott | Daniel J. Bain

Department of Geology and Environmental Science, University of Pittsburgh, Pittsburgh, Pennsylvania, USA

Correspondence
Rebecca Forgrave, SRCC 200, 4107 O'Hara St, Pittsburgh, PA 15260, USA.
Email: ref61@pitt.edu

Funding information
National Science Foundation, Grant/Award Numbers: 1253000, 1939977

Abstract

Fast hydrologic responses to storms in urban areas are often attributed to high percentages of impervious surfaces; however, another factor affecting urban storm response is channel burial. No previous studies have documented storm event responses in buried streams despite how common stream burial is in urban areas, with some US cities having over 75% of all headwater channels buried. Understanding event dynamics is particularly important as climate change predictions suggest an increase in frequency of high intensity storms and urban flooding. This study used 15-min precipitation and discharge data over a period of 6.5 years to categorize storm event responses in Nine Mile Run, an urban watershed in Pittsburgh, Pennsylvania where 98% of all channels are buried. Extensive stream burial led to lower watershed retention capacity and resulted in faster storm event responses relative to other urban streams with comparable imperviousness. Additionally, urban water subsidies in the form of sewer overflows, hydrant flushing, or water line breaks can have measurable contributions to flow event responses and result in seemingly unfeasible runoff ratios. This study demonstrates novel watershed runoff responses in systems dominated by subsurface infrastructure, which play a key role in urban water balance. Additionally, this study highlights the fact that stream restoration is not a universal solution to urban stream flashiness because downstream restoration cannot resolve the impacts of upstream burial.

KEYWORDS
buried streams, hydrograph analysis, infrastructure, rainfall-runoff responses, stormwater, urbanization

1 | INTRODUCTION

The impacts of urbanization on hydrologic response to storms are well-known: urban hydrographs are characterized by a steeper rising limb, higher peak flow, and shorter recession compared to similarly-sized rural watersheds. These impacts on flow scale with increasing watershed imperviousness and percent of landscape served by storm drainage systems. (Leopold, 1968; Schueler, 1994; Schueler et al., 2009; Shuster et al., 2005). However, stream burial, the process of relocating surface water channels into subsurface pipes, is another common characteristic of urban watersheds that has not received as much attention in terms of its effect on runoff routing and storm responses (Graf, 1975). Some buried streams are given their own pipe networks while others are deliberately captured by existing sewers (Broadhead et al., 2013).

A more precise understanding of hydrologic response to precipitation in buried streams on an event-by-event basis is important for storm water management and flood prevention (Merz et al., 2012) both now and into the future. Predicted climactic shifts will impact the hydrologic cycle both globally and locally (Kundzewicz, 2008; Trenberth, 1999) as warmer air can hold more moisture, increasing annual rainfall and the frequency of intense precipitation events

(Georgakakos et al., 2014). Due to this increased precipitation, both the overall magnitude of floods and their frequency are already increasing, and are predicted to increase further in the future (Hirsch & Archfield, 2015). Flooding in urban areas can damage buildings, roads, and other urban infrastructure (Schreider et al., 2000), as well as permanently alter ecosystems and habitat, jeopardizing the success of stream restoration projects (Bain et al., 2014).

Areas of urban land with predominantly buried surface waters have been called 'urban stream deserts' (Napieralski et al., 2015) and constitute over 11 000 km^2 of the contiguous US (Napieralski & Carvalhaes, 2016). Stream burial is more common in central portions of older North American cities, with extensive channel loss documented in Baltimore, MD (Elmore & Kaushal, 2008; Weitzell et al., 2016), Washington, DC (Weitzell et al., 2016), Cincinnati (Roy et al., 2015), Detroit, MI (Napieralski & Welsh, 2016), and Pittsburgh, PA (Hopkins & Bain, 2018). In these cities, headwaters are often preferentially buried because of their small size and spatial prevalence (Leopold, 1968).

Stream burial decreases hydrologic residence time because artificial channels and pipes are smoother and straighter than natural channels so water passes through more quickly (Henderson, 1966; Kaushal & Belt, 2012). Decreased residence time in headwater channels can result in higher flows downstream (Ogden et al., 2011), as water from more distant parts of the catchment reach the watershed outlet at the same time as nearby tributaries, Additionally, relocating stream channels to pipes complicates the connections between surface water, hyporheic zone, and riparian areas (Broadhead et al., 2013; Hopkins & Bain, 2018). Burying streams can completely separate surface water from hyporheic and soil flowpaths and prevent exchange of water. Older pipes are more likely to leak, leading to spatially heterogeneous hot-spots of infiltration and exfiltration throughout the buried drainage network (Bhaskar & Welty, 2012). The dense network of subsurface pipe conveyance created by widespread stream burial has been called 'urban karst' (Bonneau et al., 2017; Hibbs & Sharp, 2012; Kaushal & Belt, 2012). Buried pipes are often surrounded by high permeability sand and gravel that acts as a preferential flowpath for drainage of groundwater in the basin (Soulsby et al., 2014) and promote lateral movement and interactions with sewer and drinking water pipes (Sharp et al., 2003). Runoff models like SWMM do not account for pipe leakage or the preferential flowpaths around them (Bonneau et al., 2017) so the contributions from these urban water subsidies are seldom included in event studies (Bhaskar & Welty, 2012).

Watershed response to storm events can be complicated because stream discharge is a mixture of precipitation inputs and water stored in the watershed. Overland flow across impervious surfaces is the dominant transport mechanism for both water and pollutants in urban streams (Buda & DeWalle, 2009), but storm flow still contains a considerable proportion of pre-event water, ranging 20%–90%, due to groundwater travelling through urban karst (Meierdiercks et al., 2010b). Delineating the relative contribution of event and pre-event waters is challenging and there are several methods, using tracers, graphical approaches, or digital filters (Blume et al., 2007). 'Event flow' can be categorized as rainfall from a particular event, or the results of a rapid increase in hydraulic head that causes a fast release of groundwater discharge and thus a mixture of old and new water (Wittenberg, 2003). Dingman (2002) defined event flow as water volume attributable to a single event, thus, event flow includes surface runoff, interflow, sewer overflows, and fast groundwater response as a direct reaction to rainfall inputs.

Flow separation is more complex in urban systems due to contributions from combined and sanitary sewer overflows to stream discharge. Combined sewers are single pipe systems with both storm water and sanitary sewage combined in the same pipes. During flows that exceed pipe capacity, combined sewer pipe systems are designed to overflow into surface water. Separated sanitary sewers also have overflows in the case of excess pressure, which can occur when pipe capacity is exceeded from high infiltration into sewers during storm events (EPA, 2004; Pangle et al., 2022). For our purposes, both types of sewer overflows are also considered event flow because an individual overflow event is directly related to a given storm event.

To clarify patterns in buried stream event responses, we investigate the following questions in this study: How does widespread headwater stream burial affect the hydrograph response to precipitation inputs? Are there seasonal trends in the rainfall-runoff relationship? Do the thresholds of change in this relationship reveal connections among the various networks of subsurface urban infrastructure?

2 | DATA AND METHODS

2.1 | Study site

The Nine Mile Run watershed drains 15.7 km^2 of eastern Pittsburgh, PA and surrounding suburban communities. The watershed is 38% impervious surfaces and predominantly urban land cover (66%); the remainder is 18% forested, 10% grassy field, and 5% barren land (PAMAP Program Land Cover for Pennsylvania, 2005) (Figure 1b). Half of the watershed is served by combined sewers and half by separated storm and sanitary sewer networks (Figure 1c). About 60% of this sewer network in Nine Mile Run is made of vitrified clay pipe (Joe Fedor, personal communication), which commonly fails along pipe joins (Kuliczkowska, 2017). A majority of the headwaters of Nine Mile Run were buried in the 1920s (Historic Pittsburgh Maps, 2021) during a time of rapid residential development (Hopkins et al., 2013). These buried channels were often deliberately located in the same pipes as the storm sewer network (Hopkins & Bain, 2018). Today, almost all headwater channels in the Nine Mile Run watershed are buried (3 Rivers 2nd Nature, 2006), with only the most downstream portion in a restored surface channel (Figure 1b). This multi-million dollar stream restoration project was completed in 2006 and aimed to restore the main stem of Nine Mile Run, prevent erosion and flooding by connecting the stream to the adjacent floodplain wetlands, and support the recovery of instream biotic communities (Bain et al., 2014). While there were water quality and ecological improvements following restoration, this effort did not address the effects of headwater stream burial on downstream flooding.

2.2 | Data collection

We measured Nine Mile Run discharge with a HOBO pressure transducer (Onset Computer Corporation, Bourne, MA) in a stilling well installed in 2014, 300 m downstream of the culvert where the above ground portion of Nine Mile Run emerges (Figure 1). The rating curve for this pressure transducer was created with 12 paired stage-discharge measurements collected from 2014–2015 at a variety of flow conditions. The gauged reach is a concrete, trapezoidal channel, so the stage-discharge relations should remain relatively stable over time. The highest storm flow we could safely measure was 1.02 m^3/s, resulting in higher uncertainty in the stage-discharge relationship at flows above this threshold (Figure S1). The coefficient values for the rating curve were determined with an iterative non-linear least-squares regression method in R, and each have their own associated error. This uncertainty in coefficients was used to calculate a range of potential discharge values for any given stage (Figure S1). The distribution of discharge from the pressure transducer record collected for this study was comparable to the distribution of discharge data from a USGS gage (03085049, active 2006–2009) that was installed farther downstream (Kolmogorov–Smirnov test, $p < 0.0001$, Figure S2). The upstream discharge measured with the pressure transducer was often larger than the downstream discharge measured with the USGS gage due to sewer infiltration (Divers, unpublished data).

The watershed metrics calculated for this study only considered the portion of the watershed that drained directly to the gauged reach rather than the entirety of Nine Mile Run This headwater subwatershed above the pressure transducer drained a land area of 8.2 km^2, is 81% urban land use, and has 98% of all channel length buried, so it was an ideal location for investigating the effects of channel burial on storm event responses.

The buried subwatershed is served by separated storm and sanitary sewer networks. There were several gaps in the discharge record due to equipment malfunction of the pressure transducer, barometric correction station, or data shuttle, as well as the clogging of the stilling well access following a large flow event (Table 1, Figure 2). These data

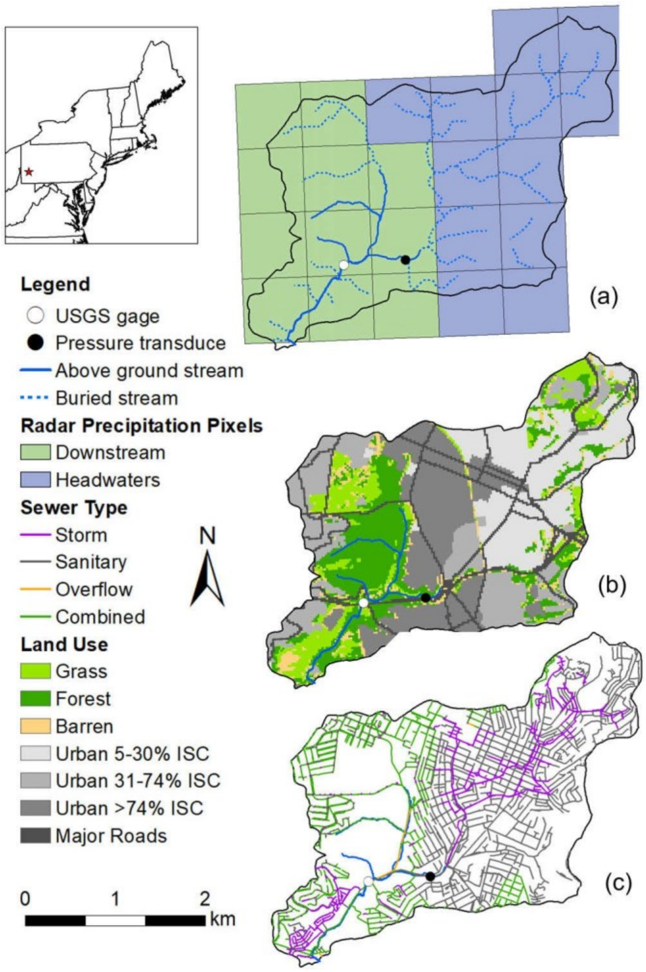

FIGURE 1 Maps of the Nine Mile Run watershed showing: (a) buried streams (dotted lines) and surface streams (solid lines) along with radar precipitation pixels designated as headwater or downstream based on the location of the discharge sensor (black dot). USGS gage installed from 2006–2009 is shown in the white dot. Map (b) shows the currently visible surface stream channels and land use from PAMAP Program Land Cover for Pennsylvania 2005. Map (c) shows the sanitary and combined sewer networks of the Nine Nile Run watershed

TABLE 1 Summary of discharge data record with data gaps and storm events by year

Year	Percentage of days missing from flow record	Number of storm events
2014	45%	47
2015	9%	81
2016	48%	36
2017	26%	79
2018	38%	68
2019	0%	126
2020	12%	88

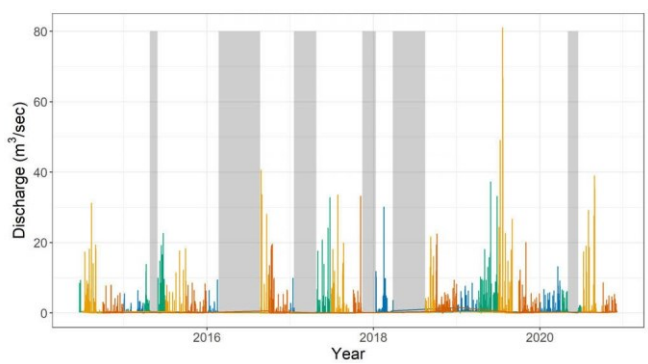

FIGURE 2 15-minute flow data time series for the entire study period (2014–2020). Gaps in data are highlighted by grey shading. Line colour designates seasons with spring in green, summer in yellow, fall in red, and winter in blue. 2019 stands out as an extremely wet with year with four of the overall 10 largest events gaps occur in all seasons but are slightly more common in spring, potentially biasing comparison of events across seasons.

Watershed precipitation data was obtained from NEXRAD radar calibrated by a network of 33 rain gages across Allegheny County (3 Rivers Wet Weather, 2021). This data included rainfall depths for every 1 km^2 grid cell in Allegheny County at 15-min intervals (Loehlein et al., 2005). For this analysis, rainfall from the 12 pixels that overlay the buried watershed (Figure 1a) was averaged to calculate a precipitation depth for each 15-min interval.

2.3 | Storm selection

The Nine Mile Run discharge data and radar precipitation data were joined into a single dataset by matching timestamp to create a 7-year record (2014–2020). We used the BaseflowSeparation function within the *EcoHydRology* R package, to separate the discharge record into 'quickflow' and 'baseflow' components using a recursive digital filter (Fuka et al., 2018), with a filter parameter of 0.99 and three passes. This filter parameter is recommended over the traditional 0.95 or 0.925 for sub-hourly time steps (Duncan, 2019; Hopkins et al., 2019) and was validated by visually inspecting hydrographs. Storm events were selected from the discharge record based on three criteria: (1) discharge greater than the threshold of 0.8 m^3/s, (2) event quickflow (Q_t) greater than 0.5 m^3/s, and (3) a discharge slope greater than a threshold slope (S_t) of 0.01 m^3/s calculated as discharge minus a 4-h leading (t_{i+4}) and 2-h lagging minimum discharge (t_{i-2}) (adapted from Hopkins et al., 2019). The thresholds were chosen to ensure that each storm was above baseflow conditions, which vary widely throughout the year. This selection process resulted in a set of 448 discharge events. Each of these identified hydrograph events were then matched with the most recent precipitation event up to 3 h before the corresponding hydrograph event. We identified precipitation events as periods of time when precipitation was greater than 0 mm, where a break in precipitation greater than 2 h was considered a separate precipitation event, resulting in a total of 1309 distinct precipitation events. There were many more precipitation events than flow events because there are no gaps in the precipitation data, and extremely small precipitation events did not produce a detectable a flow event.

In several cases ($n = 84$), multiple distinct discharge peaks were classified as the same event because the stream did not return to baseflow conditions before the next precipitation event created a discharge response. These were manually separated at each streamflow minima. In sum, a total of 525 matching discharge and precipitation events were used in the following analyses. For seasonal analyses, spring is March 20th–June 19th, summer is June 20th-September 21st, fall is September 22nd–December 20th, and winter is December 21st–March 19th.

2.4 | Event metrics and statistics

For each paired precipitation-discharge event, the precipitation metrics calculated included: total event precipitation depth (mm), precipitation event duration (h), precipitation intensity (mm/h), and 5-day total antecedent precipitation depth (mm). For all precipitation metrics, only the buried watershed area above the pressure transducer was considered. We chose 5-day antecedent precipitation as a measure of antecedent conditions because it is more directly comparable to flow metrics than measurements of soil moisture (Smith et al., 2013). The hydrologic response variables were hydrograph peak duration (h), maximum discharge (m^3/s), runoff yield (total runoff volume converted to a depth by dividing by watershed area) (mm), and the hydrograph rise time (hours from start of hydrograph event to peak of discharge).

To evaluate the relationships between precipitation and discharge events, we calculated runoff ratio and lag time. Runoff ratio, also called runoff coefficient, is a unitless volume ratio of event rainfall to either total flow volume or quickflow volume (Blume et al., 2007). Runoff ratio can be calculated in an annual or event basis. Since this paper focuses on events, we calculate runoff ratio as total quickflow divided by total event rainfall for each event. Lag time is the amount of time between the precipitation event and hydrograph event. It is often calculated as the hours between the centroid of precipitation and the maximum discharge (Smith et al., 2013), but for some events with very fast watershed responses and extended precipitation, the maximum flow occurred before the centroid of precipitation which would result in a negative lag time, so we chose to use the time between the start of precipitation and start of the hydrograph rise.

We assessed correlations between maximum discharge, runoff yield, and event precipitation using simple linear regression performed in R. Except for runoff ratio, all precipitation and discharge response variables were log transformed for linear regressions. Runoff ratio is approximately normal without transformation. While log transformed data are not statistically normal, they do follow an approximate Gaussian shape, with the exception of streamflow rise time (Figure 3). Rise time is limited by the 15-min data collection interval, so anything faster than 15-min will appear in the data as a 0-min rise time, and thus be removed from log-transformed data. Seasonal variation in both the precipitation input and watershed response metrics listed above were assessed with ANOVAs and Tukey's post-hoc tests performed in R.

3 | RESULTS

3.1 | Precipitation events and hydrologic responses

Over the full study period from 2014–2020, there were 525 distinct storm events that met the criteria defined above (Figure 2, Table 2). 2019 was the wettest year during the study period with a total of 1328 mm of precip from 130 storm events and was also the only year in the record with no data gaps (Table 1). Total event precipitation depth ranged from 0.24 to 181.7 mm, and event duration spanned from 0.25 to 63.5 h. Precipitation event intensity ranged from 0.2 to 45.4 mm/h. The 5-day antecedent precipitation depth prior to event onset ranged from 0.0 to 87.5 mm. In terms of event responses,

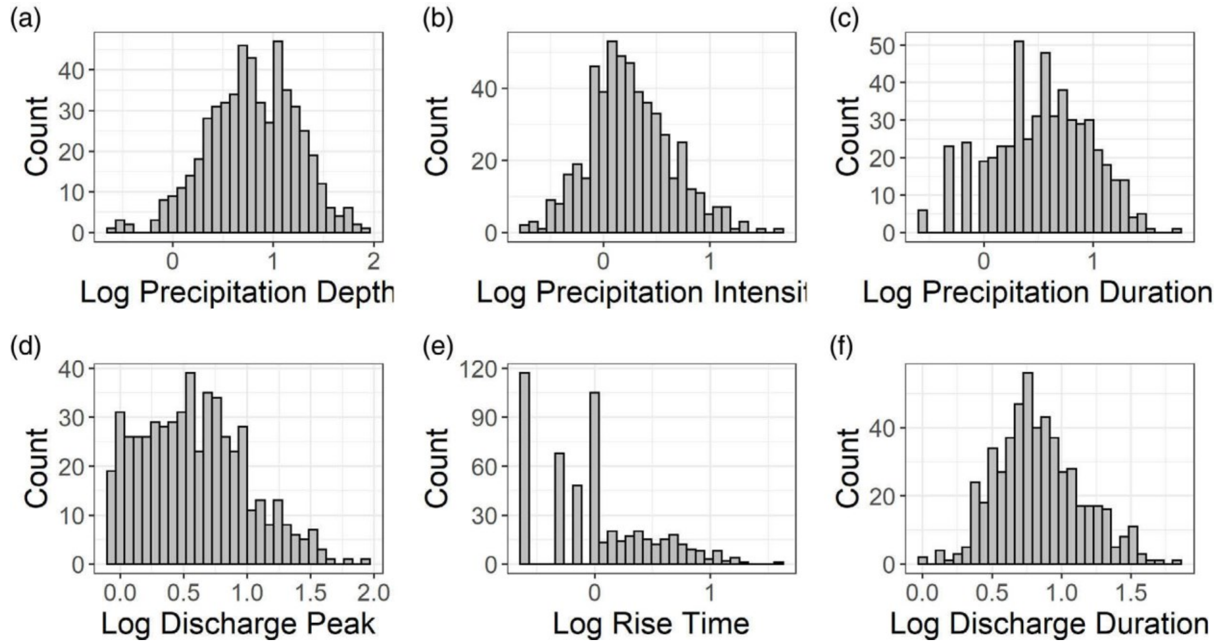

FIGURE 3 Histograms of log transformed data: (a) precipitation depth, (b) precipitation intensity, (c) precipitation duration, (d) peak discharge, (e) hydrograph rise time, and (f) discharge duration. All distributions except rise time are approximately normal, though they are all statistically different from normal due to the influence of a few outliers (Shapiro–Wilk test, precipitation depth: $p = 0.0036$, precipitation intensity: $p = 0.0027$, precipitation duration: $p = 0.0019$, discharge peak: $p < 0.0001$, rise time: $p =$ NA, discharge duration: $p = 0.0008$)

TABLE 2 Summary statistics of event metrics

	Mean	Median	Minimum	Maximum
Precipitation metrics				
Total event precipitation (mm)	10.22	6.32	0.24	181.67
Precipitation duration (h)	5.62	3.75	0.25	63.50
Precipitation intensity (mm/h)	2.76	1.64	0.18	45.38
5-day antecedent precip (mm)	16.75	13.23	0.00	87.47
Hydrograph response metrics				
Peak discharge (m^3/s)	6.13	3.65	0.81	81.05
Hydrograph event duration (h)	9.02	6.25	1.00	81.50
Runoff yield (mm)	5.02	2.49	0.24	124.56
Rise time (h)	1.92	0.75	0.00	39.50
Combined metrics				
Lag time (peak starts) (h)	2.11	1.75	0.00	13.00
Runoff ratio	0.46	0.42	0.10	3.14

discharge events spanned between 1.0 and 81.5 h in duration. Lag times between the start of the precipitation event and the start of the discharge event ranged from 0.0 to 13.0 h with a median of 1.8 h. Hydrograph rise time ranged from 0.0 to 39.5 h with median of 0.75 h. Measurement of response time is fundamentally limited by the data collection interval (15 min). There were 24 events where the rise time from the start of hydrograph rise to its peak was 15 min or less, meaning that the entire hydrograph rise occurred between data collection points. These extremely fast storms have hydrograph rise ranging from 14.1 to 40.6 m^3/s in that 15-min interval. Peak discharge ranged from 0.81 to 81.1 m^3/s. This highest flow is 400x the average baseflow condition of 0.2 m^3/s. For these extremely high peaks, the error of the coefficients of the stage-discharge curve means the 81.1 m^3/s peak flow could be anywhere between 55.3 and 110.1 m^3/s.

3.2 | Relationships among the precipitation and streamflow metrics

In general, longer precipitation events led to longer flow events ($R^2 = 0.605$, $p < 0.001$). A higher precipitation depth led to both higher peak streamflow ($R^2 = 0.523$, $p < 0.001$, Figure 4a) and a larger runoff yield ($R^2 = 0.889$, $p < 0.001$, Figure 4d). Although higher precipitation intensity resulted in higher peak streamflow ($R^2 = 0.526$, $p < 0.001$, Figure 4b), the relationship between precipitation intensity and runoff yield was weak ($R^2 = 0.142$, $p < 0.001$, Figure 4e). These relationships are affected by the presence of a few storms with very high flows, or very low precipitation, but are not considered outliers (Rosner's test in the *EnvStats* R package) and are thus not excluded from the analysis. Neither peak streamflow nor runoff yield were correlated with 5-day antecedent precipitation (Figure 4c,f) and thus indicated that pre-event water plays a negligible role in determining event response.

3.3 | Seasonal variation in watershed response

Throughout the study period, summer had the highest total number of storms ($n = 167$), followed by fall ($n = 137$), spring ($n = 123$), whereas winter had the fewest storms ($n = 99$). However, there were several month-long gaps in the flow data that could affect these numbers. While days without data occurred in all seasons, the majority of them (56%) occurred in spring and fewest in fall (5%) (Figure 2), so spring storms will be slightly underrepresented in this analysis compared to their actual frequency. To illustrate this point, if we consider only years where <15% of the flow data is missing (2015, 2019, and 2020), the greatest number of storms was in the spring or summer, followed by winter or fall.

The average event precipitation depth for each season was within 3.2 mm of each other (winter = 10.4 mm, spring = 8.3 mm, summer = 9.4 mm, and fall = 11.5 mm), and there was a significant difference between precipitation depth in both spring and summer (drier) and fall (wetter) seasons (Tukey's test, $p = 0.02$ for spring–fall, $p = 0.04$ for summer–fall, Figure 5a). These seasonal differences in precipitation were more apparent in precipitation event duration. Pittsburgh has a humid climate that experiences convective thunderstorms in the late spring and summer. These thunderstorms storms deliver similar amounts of precipitation in a shorter time interval, averaging 3.3 and 4.2 h for spring and summer, relative to 7.6 and 8.3 h for fall and winter (ANOVA, $p < 0.001$, Table 3, Figure 5b). The shorter duration summer and spring precipitation events lead to significant differences in precipitation intensities with an average intensity of 4.5, 2.6, 1.9, and 1.2 mm/h for summer, spring, fall, and winter, respectively (ANOVA, $p < 0.001$, Table 3, Figure 5c).

This intense precipitation in summer and spring led to rapid and high discharge responses. The average summer hydrograph peak (9.2 m^3/s) is nearly twice as large as in fall (4.6 m^3/s) and winter (3.8 m^3/s). Summer discharge peaks were significantly higher compared to fall and winter (Tukey's test, $p < 0.001$ for summer–winter, $p < 0.001$ for summer–fall) and spring was significantly higher than winter (Tukey's test, $p = 0.005$, Figure 5f). Spring and summer

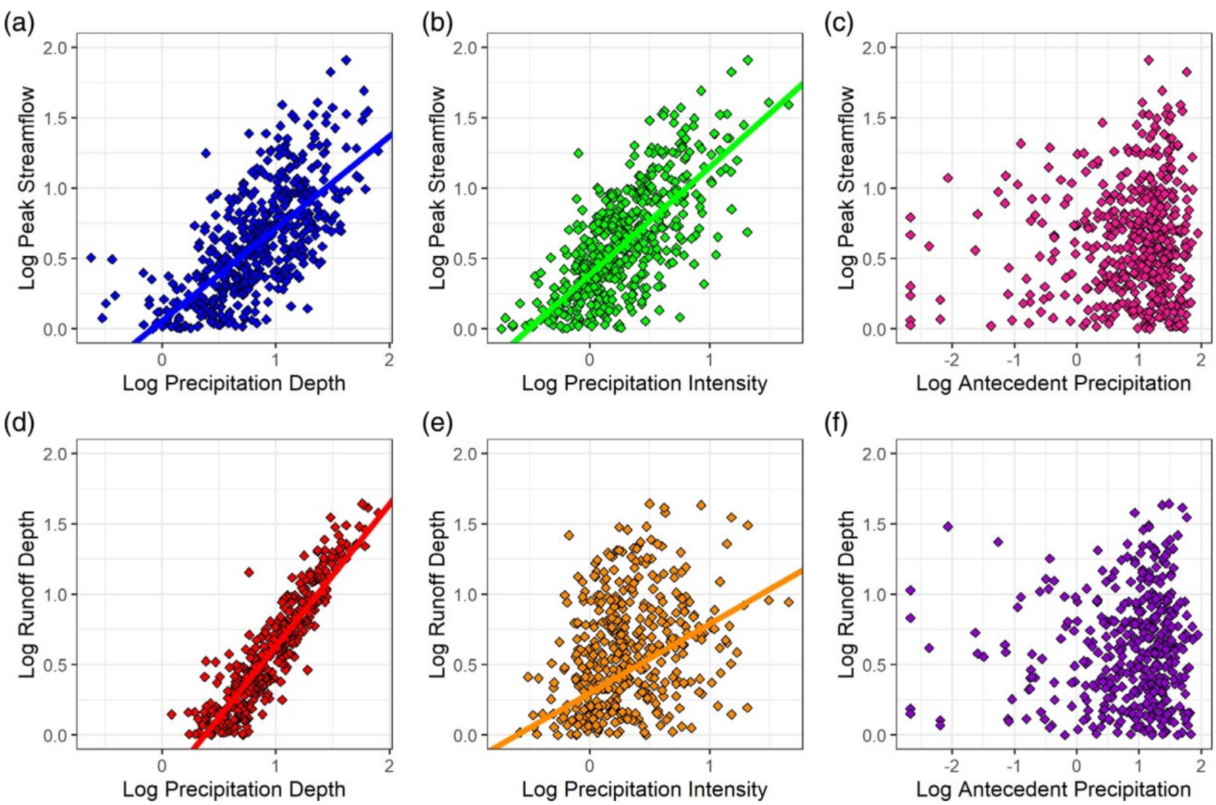

FIGURE 4 Linear regressions showing relationships among log-transformed precipitation and hydrograph response variables. Each data point is a storm event, and the line shows the linear regression.

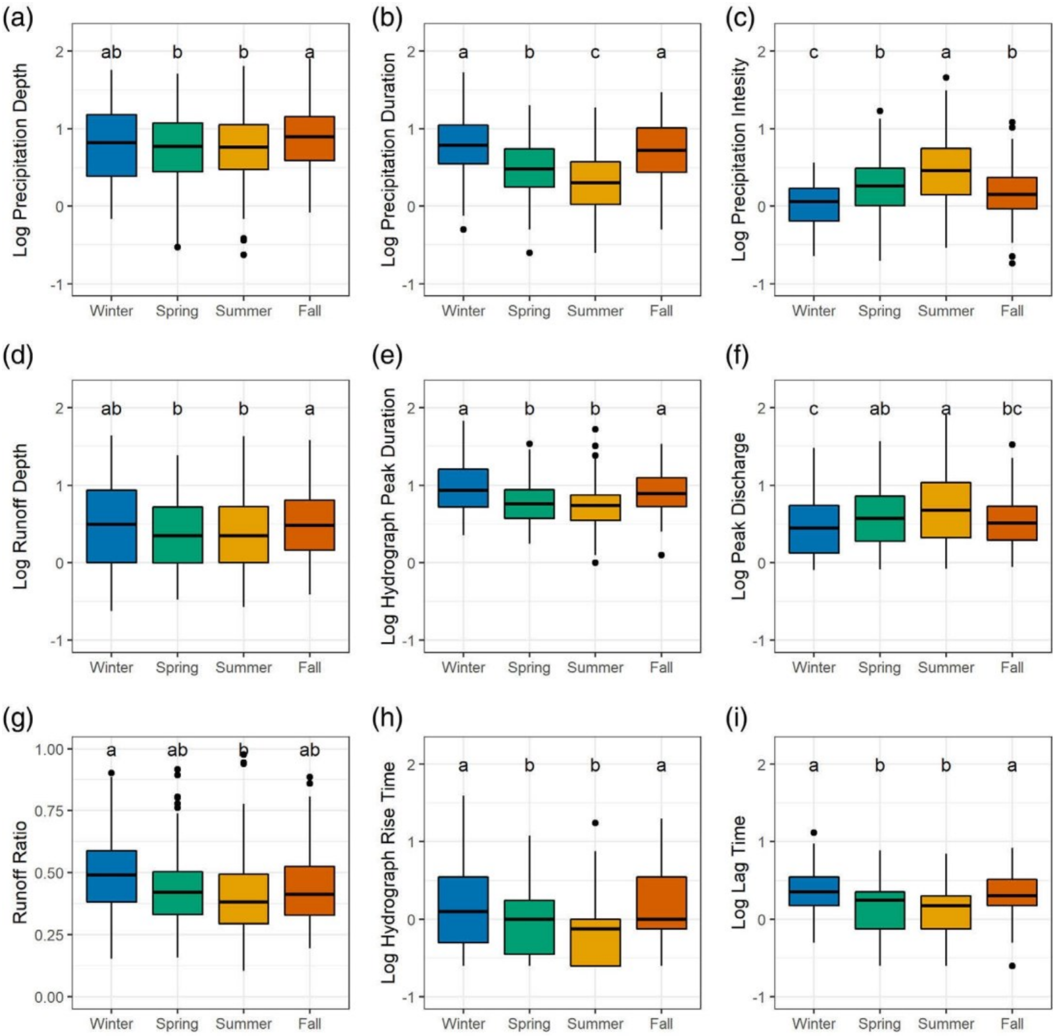

FIGURE 5 Seasonal differences in event metrics: (a) event precipitation, (b) precipitation intensity, (c) precipitation duration, (d) runoff depth, (e) peak discharge, (f) hydrograph peak duration, (g) runoff ratio, (h) hydrograph response time, and (i) lag time. All metrics except runoff ratio are log-transformed. Letters indicate significant differences from Tukey's post-hoc comparison. Events with runoff ratios greater than 1 are not shown

TABLE 3 Average event metrics separated by season

Event metric	Winter	Spring	Summer	Fall
Event precipitation (mm)	10.37	8.24	10.44	11.46
Precipitation intensity (mm/h)	1.24	2.60	4.48	1.92
Precipitation duration (h)	8.26	4.17	3.39	7.63
Runoff depth (mm)	5.97	3.69	5.19	5.34
Flow peak (m^3/s)	3.80	5.84	9.20	4.59
Flow peak duration (h)	12.38	7.43	7.07	10.48
Runoff ratio	0.55	0.47	0.48	0.46
Rise time (h)	3.04	1.28	1.10	2.61
Lag time (h)	2.73	1.76	1.61	2.51

discharge events were both of significantly lower duration (Tukey's test, $p < 0.001$ relative to summer–winter, summer–fall and spring–winter, $p = 0.001$ for spring–fall, Figure 5e). This reflects the fact that spring and summer storms tend to be a single discharge peak followed by a recession, whereas longer-duration storms in fall and winter often have multiple peaks in response to individual pulses of precipitation inputs, leading to an overall longer time above baseflow conditions. Discharge rose more quickly in summer and spring, 1.1 and 1.3 h, respectively, compared to 2.6 h for fall and 3.0 h for winter (Tukey's test, $p < 0.001$ for summer-winter and summer-fall, $p = 0.003$ for spring-winter, and $p = 0.002$ for spring-fall, Figure 5h). The lag time between precipitation and flow events also followed this same pattern of shorter in summer and spring than fall and winter (Tukey's test, $p < 0.001$ for summer-winter, summer-fall, spring-winter, and spring-fall, Figure 5i).

3.4 | Runoff ratios

The average event-specific runoff ratio across the full dataset was 0.48 ± 0.27. The average value for winter (0.50 ± 0.17) was slightly higher than the other seasons (spring = 0.47 ± 0.23, summer = 0.48 ± 0.37, fall = 0.46 ± 0.23), but this difference was not significant (ANOVA, $p = 0.22$, Figure 5g). The high standard deviation shows considerable variation in runoff ratios among events. However, almost none of the observed variability in runoff ratios can be explained by log-transformed event precipitation (linear regression, $R^2 = 0.003$, $p = 0.003$), precipitation intensity ($R^2 = 0.002$, $p = 0.13$), or pre-event discharge ($R^2 = 0.056$, $p < 0.001$).

3.5 | Time lags between precipitation and streamflow

Across all events, the lag time between the start of the precipitation and start of the hydrograph event was an average of 2.1 h, but it ranged from less than 15 min up to 13 h. There were 70 events with a lag time of 30 min or less, showing the Nine Mile Run system is extremely reactive to rainfall. One example of these storms with a 15-min lag time is shown in Figure 6.

4 | DISCUSSION

4.1 | Buried streams are the flashiest urban streams

Although urban streams are often described as 'flashy', characterized by faster hydrograph rise and fall than rural reference streams (Walsh et al., 2005), the widespread channel burial in Nine Mile Run makes it respond faster and with a larger peak discharge per square kilometre of drainage area than most other urban streams (Table 4). Throughout the literature, hydrograph 'flashiness' has had several definitions

TABLE 4 Summary of watershed flashiness in this study and other urban streams in the literature

Metric defining 'flashiness'	This study (buried stream)	Other urban streams
Fast watershed response time/lag time	Average of 79 min	Average of 102 min (Smith et al., 2013)
Short hydrograph rise time	Average of 45 min	Less than 1 h (Smith et al., 2013)
Frequent high flow events	Average of 16.7 events/year over 1 $m^3/s/km^2$	12 events/year over 1 $m^3/s/km^2$ (Smith, Miller, et al., 2005)
Short duration of elevated flow conditions	24% of the record over mean flow	30% of total time above mean flow (Konrad et al., 2005)

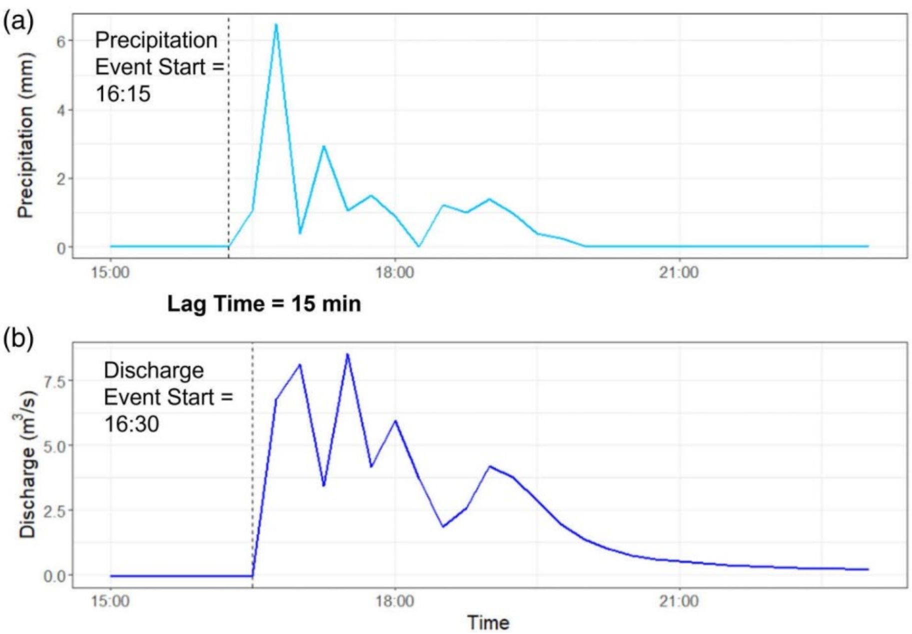

FIGURE 6 Precipitation and discharge time series for one example storm to illustrate the short lag time between the start of the precipitation event and the start of the rise in discharge. This event is from 15:00-23:00 on July 7, 2017

based on fast watershed response time (Smith et al., 2013), high rate of change in hydrograph on both rising and falling limbs (McMahon et al., 2003; Poff et al., 1997), the short duration of elevated flow conditions (Konrad et al., 2005; McMahon et al., 2003), or high frequency of events over a specific threshold (Smith et al., 2013; Smith, Miller, et al., 2005).

In the context of flashiness reported for urban streams, the largest 50 events recorded in Dead Run (30% impervious) in Baltimore from January 2000–December 2009 had an average watershed response time, also known as lag time, of 102 min from the time of the rainfall centroid to the peak discharge (Smith et al., 2013). In contrast, in Nine Mile Run (38% impervious), the largest 50 events have an average lag time of 41 min from centroid of precipitation to flow peak (Figure 6). This number is complicated by the fact that nine of these storms have negative lag times using this approach, where the peak discharge occurs before the bulk of precipitation has occurred, due to an extremely fast hydrograph rise. For this reason, we chose to use the time between precipitation start and start of hydrograph rise as the lag time for all events. Using this approach, the watershed response time of the largest 50 storms events averages 79 min, still 22% faster than Dead Run. The short lag times in urban watersheds are due to impervious surfaces that prevent infiltration and engineered drainage systems that efficiently route runoff to streams. This drainage efficiency means that rain falling in the headwater can reach the watershed outlet almost as fast as rain falling adjacent to the channel. In general, event lag times scale with the percent impervious cover (Meierdiercks et al., 2010b). However, as demonstrated in this study, stream burial further accelerates the short lag times of urban streams due to the integration of surface, soil, and pipe flowpaths that routes all water in pipe networks engineered to conduct water as fast as possible. As a result, any precipitation in the Nine Mile Run watershed reaches the stream via the fastest route possible soon after the storm begins.

In contrast to lag times that include both the time for rain to become runoff and travel times through watershed flowpaths, hydrograph rise time—the amount of time between when stream discharge starts to rise and when it reaches peak discharge—only reflects runoff travel times. The median hydrograph rise time in Nine Mile Run for all events was 45 min, but there are 28 events with a rise time of 15 min or less. This rise time is comparable to urban watersheds in the Baltimore area where six watersheds have hydrograph rise times of less than an hour and three of them are less than 15 min, (Smith et al., 2013). One notable difference is that the Baltimore study only quantifies the 50 largest storm events in a 10-year period for each watershed, whereas we characterize the median rise time for this study based on all events in a 6.5-year period. In Baltimore, rise times were not related to land use, but time period of urban development and presence of stormwater detention infrastructure (Smith et al., 2013). In contrast, buried streams have no stormwater detention facilities and instead conduct all stormwater to the stream as fast as possible, explaining the extremely fast rise times. A study of urban and suburban watersheds in New York state found a decrease in rise times with urbanization that is closer to the watershed outlet as opposed to farther away in the headwaters (Roodsari & Chandler, 2017) but this spatial organization of landscape impacts is less relevant when the stream is fully-buried, because all flowpaths are artificial drainages and travel times from the headwaters to the outlet are extremely fast.

The rapid hydrograph rise time in urban streams translates to a shorter overall time in elevated flow conditions compared to rural streams (McMahon et al., 2003). In Nine Mile Run, there were 58 events where the entire hydrograph rise and recession occur in less than 3 h. These quick events had some large flows: one event rose up to 18 m^3/s and back down to 0.3 m^3/s in less than 3 h. The overall impact of fast hydrograph changes can be quantified by comparing the percentage of time that a stream exceeds its mean streamflow over long time periods (Konrad et al., 2005). For example, urban streams in the Puget Sound region of Washington State had less than 30% of the total time above mean flows (Konrad et al., 2005). During the study period, Nine Mile Run is similar with flows exceeding the mean discharge only 24% of the total record.

The frequency of rapid storm response is also indicative of stream flashiness. Moores Run in Baltimore (9.1 km^2) has been reported as one of the flashiest streams in the contiguous US based on a 10-year dataset with an average of 12 events per year when discharge exceeded 1 $m^3/s/km^2$ (Smith, Miller, et al., 2005). These frequent high flows are attributed to high urbanization (82% urban land use), stream burial in the upper watershed, efficient concentration of runoff in the storm drain network, and a lack of stormwater detention structures (Smith et al., 2013; Smith, Miller, et al., 2005). The Nine Mile Run buried subwatershed, which is a comparable size (8.2 km^2) and urbanization (81% urban land use), had 117 total events exceeding this same discharge threshold of 1 $m^3/s/km^2$ threshold in 6.5 years of data with an average of 16.7 events per year. The frequency of fast storm responses in these two extremely impacted urban watersheds supports the role of stream burial in generating flashy storm response. Most discussions of flashy urban streams have focused on urban watersheds where total imperviousness or connected imperviousness is a primary driver of fast storm responses, whereas Hopkins et al. (2015) emphasized the importance of regional physiographic characteristics in determining the relationship between urban development and high flows. Catchments with shallower slopes, higher soil permeability, and more lakes, such as Boston, MA; Detroit, MI; Portland, OR; and St. Paul, MN can buffer the impacts of urbanization and generally have lower peak flows compared to cities in areas with higher slopes or less permeable soils including Pittsburgh, PA; Atlanta, GA; and Raleigh, NC (Hopkins et al., 2015). Conversely, Roodsari and Chandler (2017) found that when comparing watersheds within a single region, catchment morphology, hydraulics, topography, and soils were less correlated with runoff peak flows and stream flashiness than the percentage of artificial pathways in the watershed. This study supports both of these previous studies and demonstrates that in addition to regional physiographic characteristics, the type of urban development also impacts event responses. The Nine Mile Run subwatershed has steep slopes, impermeable soils, but also is composed of 98% buried channels. This dominance of stream burial creates a system where streamflow responses are higher, faster, and more frequent than other urban watersheds of comparable size, imperviousness, and underlying geology.

4.2 | Dominance of convective summer thunderstorms in climate-driven flooding

Throughout the study period, convective summer thunderstorms dominated the overall watershed response. These storms are intense localized storms triggered by the vertical movement of heat and moisture and characterized by heavy rain, thunder, lighting, strong winds, and sudden changes in temperature (Smith, Baeck, et al., 2005; Smith, Miller, et al., 2005). Intense summer storms dominated overall storm response trends because of the high discharge peaks, short duration, and small spatial area (Figure 5b,c), and also because summer had, on average, more storm events than other seasons. While this finding in itself is not new (Valtanen et al., 2014; Yang et al., 2013), it is important because warm season thunderstorms are the primary mechanism of flashy floods in urban environments (Ntelekos et al., 2008; Smith, Baeck, et al., 2005; Smith, Miller, et al., 2005). These summer rainfall events are predicted to become more intense in next decades as warmer air temperatures lead to a higher frequency of intense storms (Drum et al., 2017; Hirsch & Archfield, 2015). Urban areas can even increase likelihood of thunderstorms because the urban heat island effect can create convergence zones above and downwind of the urban area, as well as the increased concentration of aerosols from emissions can increase rainfall and streamflow in urban streams (Bornstein & Lin, 2000; Ntelekos et al., 2008). This climatic pressure will be even more apparent in watersheds with buried streams because the pipes that contain buried streams were built to accommodate the stream flow of 100 years ago, whereas increased runoff from development and climate change leads to stream flows that exceed pipe capacity. Urban stream deserts with no surface stream channels due to complete burial, which comprise the 6% of all urban land across the continental U.S., are more likely to flood, potentially affecting up to 73 million people (Napieralski & Carvalhaes, 2016).

4.3 | Runoff ratios reflect water subsidies from failing urban infrastructure

Runoff ratios describe how landscapes transform rainfall inputs into runoff that contributes to streamflow (Blume et al., 2007) where high values can indicate higher risk of surface floods. The average annual runoff ratio is 0.46 for Nine Mile Run and reveals that for a typical event, half of the event rainfall becomes runoff in the stream. The other half infiltrates into soil, groundwater, or buried pipe infrastructure, where it is released back into the stream after the event or lost to evapotranspiration. In the case of pipe infiltration, water can also be transported to other watersheds via sanitary sewer networks. Despite seasonal variation in precipitation amounts and hydrograph responses, event runoff ratios are consistent throughout the year (Figure 5g), suggesting that this metric reflects the effects of urban infrastructure on flow routing rather than any hydroclimate pattern.

Runoff ratios are usually related to antecedent rainfall (Haga et al., 2005; Smith, Baeck, et al., 2005; Smith, Miller, et al., 2005). For example, when a watershed is more saturated from past rainfall inputs, more rainfall is converted to event runoff. This relationship of runoff ratios with watershed saturation is also seasonal, with slightly higher runoff ratios in winter when there is more storage of water in the catchment due to decreased evapotranspiration losses. Event runoff ratios in Dead Run and Moores Run, both urban streams in Baltimore, ranged 0.38–0.88 and had a positive relationship with total event rainfall and antecedent moisture conditions However, event runoff ratios in Nine Mile Run are also not related to event precipitation inputs or antecedent moisture, suggesting that due to channel burial and rapid routing of runoff, there is minimal watershed storage of event water between events to affect the runoff ratio of the next event.

During the study period, 14 storm events had a runoff ratio greater than 1, meaning that there is more event water in the stream than precipitation inputs. We initially thought this was due to accumulated responses to multiple, closely-timed storms that confounded runoff accounting among events. Even after these events ($n = 6$) were eliminated, there are eight other events, all in the summer, with runoff ratios greater than 1. This 'water subsidy' could be from sewer overflows, hydrant flushes, or water line breaks. While the uncertainties in the stage-discharge relationship (Figure S1) can affect calculation of event runoff ratios, even with the lowest possible discharge from the stage-discharge relationship, there are still multiple events with runoff ratios exceeding 1. The phenomenon of urban water subsidies has been considered in other urban hydrology studies (Bhaskar & Welty, 2012; Kaushal & Belt, 2012; Pangle et al., 2022) and warrants further exploration, particularly because these subsidies are heterogenous in space and time. Pipe leakage is not evenly distributed around a watershed but concentrated in certain places (Bhaskar & Welty, 2012), and new fractures can form due to changes in weather, or old fractures can be repaired or blocked with debris and stop leaking (DeSilva et al., 2005), making attribution to one particular urban water source challenging. The likelihood of sewer overflows in Nine Mile Run is high due to proximity of sewage pipes—a large (1.4 m diameter) collector sewer pipe runs alongside the mainstream channel for its entire length—and advanced sewer age of this network (~100 years old) (Divers et al., 2013). While sanitary sewers are not designed to receive storm water, old pipes are subject to fractures, failures, and intrusion by tree roots that introduce opportunities for groundwater to infiltrate through pipe cracks and create flows that exceed pipe capacity. We have observed sanitary sewers overflowing through utility access points into the stream during many storm events. Inflow and infiltration of freshwater into sanitary sewers can constitute 20%–50% if the total flow (Bareš et al., 2012; Karpf & Krebs, 2011; Kracht et al., 2007; Kracht & Gujer, 2005; Pangle et al., 2022), and is the dominant cause of sanitary sewer overflows (EPA, 2004).

The remaining eight storms with runoff ratios greater than one fall into three groups based on the magnitude of the discharge peak: discharge peak less than 2 m^3/s, discharge peak 2–4 m^3/s, and discharge peak above 4 m^3/s. For the four storms below 2 m^3/s, we attribute the high runoff ratios (1.1–1.7) to water infrastructure failures such as drinking water main breaks and hydrant flushing. These storms all have low event precipitation (0.3–0.4 mm) that cannot account for the size of the discharge peaks (1.0–1.7 m^3/s), so the high runoff ratio could be due to the contribution of anthropogenic sources of water in the watershed. The two storms with discharge peaks of between 2 and 4 m^3/s also have low event precipitation (0.2 and 0.4 mm) but have high antecedent precipitation (6.5 and 15.7 mm), suggesting that higher soil saturation, and sewer pipes at higher capacity from previous storms may create favourable conditions for sanitary sewer overflows and lead to the observed event runoff ratios of 2.0 and 3.2, respectively. In the last case, the two storms with very high discharge peaks (17.7 and 24.4 m^3/s) have both high event precipitation and high antecedent precipitation, suggesting event precipitation filled pipes beyond capacity.

All storms with runoff ratios greater than one occurred in summer or the very end of spring, further supporting the role of high intensity convective thunderstorms for triggering sewer overflow events, especially when there are multiple consecutive high-intensity events in the watershed over several days. These overflow-driven streamflow subsidies are spatially heterogenous, and infrequent, but can still affect the hydrology, especially in a stream that is as responsive to storm drainage inputs as Nine Mile Run.

5 | CONCLUSIONS

While Nine Mile Run is comparable in size and imperviousness to many prominent urban watershed case studies (Konrad et al., 2005; Meierdiercks et al., 2010a; Smith et al., 2013; Smith, Miller, et al., 2005), it is considerably flashier by almost all metrics. We attribute this to the widespread (98%) stream burial of Nine Mile Run stream channels. The inconsistent linkage between flow events and antecedent precipitation, and the narrow range of runoff ratios observed throughout the year seem to result from the dominant piped drainage. Runoff ratios greater than one suggest considerable infrastructure failures and highlight the importance of urban water subsidies, such as sewer overflows and water main breaks, as important contributors to urban streams during storm events, especially those when systems are at capacity from previous storms.

We observed the largest and fastest event responses to convective summer thunderstorms, and it is these high intensity storms that are predicted to increase in frequency over the next several decades (Hirsch & Archfield, 2015). It is essential to support projects that build watershed retention capacity and mitigate the effects of urban flooding. However, this is no easy task. For example, while some studies show stormwater detention decreases peak flows (Pennino et al., 2016), other studies determined that the presence of stormwater management facilities have an negligible effect on reducing peak flows or discharge rise time (Miller et al., 2021). Our study results further underline limitations inherent in using stream restoration projects as end-of-pipe solutions to flashy urban streams. Hydrologic responses driven by buried headwaters can threaten the success of restoration projects when flows exceed design flows and wash out wetlands, riparian areas, and other habitat restoration interventions (Bain et al., 2014).

ACKNOWLEDGEMENTS

This material is based upon work supported by the National Science Foundation under Grant Nos. 1939977 and 1253000 to EM Elliott. This work was also supported by the Pittsburgh Water Collaboratory and the Mellon Pre-Doctoral Fellowship at the University of Pittsburgh. We would also like to thank Sarah Lavin for establishing the gage and developing early stage-discharge relationships, Joe Fedor for downloading stage data and sharing sewage pipe flow data and Krissy Hopkins for sharing her event selection code. We appreciate the comments and suggestions from Dr. Sarah Ledford and two anonymous reviewers for their improvement of the manuscript.

DATA AVAILABILITY STATEMENT

Radar precipitation data for Allegheny County can be downloaded from https://www.3riverswetweather.org/municipalities/calibrated-radar-rainfall-data. Nine Mile Run discharge data and analysis scripts can be made available upon request to ref61@pitt.edu.

ORCID

Rebecca Forgrave https://orcid.org/0000-0001-7240-6569

REFERENCES

3 Rivers 2nd Nature. (2006). Allegheny County: Landscape Ecology and Green Infrastructure. https://www.pasda.psu.edu/uci/DataSummary.aspx?dataset=1251

3 Rivers Wet Weather (2021). *Calibrated radar rainfall data*. https://www.3riverswetweather.org/municipalities/calibrated-radar-rainfall-data

Bain, D. J., Copeland, E. M., Divers, M. T., Hecht, M., Hopkins, K. G., Hynicka, J., Koryak, M., Kostalos, M., Brown, L., Elliott, E. M., Fedor, J., Gregorich, M., Porter, B., Smith, B., Tracey, C., & Zak, M. (2014). Characterizing a major urban stream restoration project: Nine mile run (Pittsburgh, Pennsylvania, USA). *Journal of the American Water Resources Association*, *15*, 218–1621. https://doi.org/10.1111/jawr.12225

Bareš, V., Stránský, D., & Sýkora, P. (2012). Evaluation of sewer infiltration/inflow using COD mass flux method: Case study in Prague. *Water Science and Technology*, *66*(3), 673–680. https://doi.org/10.2166/wst.2012.229

Bhaskar, A. S., & Welty, C. (2012). Water balances along an urban-to-rural gradient of metropolitan Baltimore, 2001–2009. *Environmental and Engineering Geoscience*, *18*(1), 37–50. https://doi.org/10.2113/gseegeosci.18.1.37

Blume, T., Zehe, E., & Bronstert, A. (2007). Rainfall-runoff response, event-based runoff coefficients and hydrograph separation. *Hydrological Sciences Journal*, *52*(5), 843-862. https://doi.org/10.1623/hysj.52.5.843

Bonneau, J., Fletcher, T. D., Costelloe, J. F., & Burns, M. J. (2017). Stormwater infiltration and the 'urban karst' – A review. *Journal of Hydrology*, *552*, 141–150. https://doi.org/10.1016/j.jhydrol.2017.06.043

Bornstein, R., & Lin, Q. (2000). Urban heat islands and summertime convective thunderstorms in Atlanta: Three case studies. *Atmospheric Environment*, *34*(3), 507–516. https://doi.org/10.1016/S1352-2310(99)00374-X

Broadhead, A. T., Horn, R., & Lerner, D. N. (2013). Captured streams and springs in combined sewers: A review of the evidence, consequences and opportunities. *Water Research*, *47*(13), 4752–4766. https://doi.org/10.1016/j.watres.2013.05.020

Buda, A. R., & DeWalle, D. R. (2009). Dynamics of stream nitrate sources and flow pathways during stormflows on urban, forest and agricultural watersheds in Central Pennsylvania, USA. *Hydrological Processes*, *23*(23), 3292–3305. https://doi.org/10.1002/hyp.7423

DeSilva, D., Burn, S., Tjandraatmadja, G., Moglia, M., Davis, P., Wolf, L., Held, I., Vollertsen, J., Williams, W., & Hafskjold, L. (2005). Sustainable management of leakage from wastewater pipelines. *Water Science and Technology*, *52*(12), 189–198. https://doi.org/10.2166/wst.2005.0459

Dingman, S. L. (2002). *Physical hydrology* (p. 646). Prentice Hall.

Divers, M. T., Elliott, E. M., & Bain, D. J. (2013). Constraining nitrogen inputs to urban streams from leaking sewers using inverse modeling: Implications for dissolved inorganic nitrogen (DIN) retention in urban environments. *Environmental Science and Technology*, *47*(4), 1816–1823. https://doi.org/10.1021/es304331m

Drum, R. G., Noel, J., Kovatch, J., Yeghiazarian, L., Stone, H., Stark, J., Kirshen, P., Best, E., Emery, E., Trimboli, J., Arnold, J., & Raff, D. (2017). *Ohio River Basin: Formulating climate change mitigation/adaptation strategies through regional collaboration with the ORB alliance*. Civil works technical report, CWTS 2017-01. Alexandria, VA: U.S. Army Corps of Engineers, Institute for Water Resources (Issue May). http://www.lrh.usace.army.mil/Portals/38/docs/orba/USACE%20Ohio%20River%20Basin%20CC%20Report_MAY%202017.pdf

Duncan, H. P. (2019). Baseflow separation – A practical approach. *Journal of Hydrology*, *575*, 308–313. https://doi.org/10.1016/j.jhydrol.2019.05.040

Elmore, A. J., & Kaushal, S. S. (2008). Disappearing headwaters: Patterns of stream burial due to urbanization. *Frontiers in Ecology and the Environment*, *6*(6), 308–312. https://doi.org/10.1890/070101

EPA (2004). *Report to congress on impacts and control of combined sewer overflows and sanitary sewer overflows*. https://www.epa.gov/npdes/2004-npdes-cso-report-congress

Fuka, D., Walter, M., Archibald, J., Steenhuis, T., & Easton, Z. (2018). *EcoHydRology, R Package*. CRAN. https://cran.r-project.org/web/packages/EcoHydRology/EcoHydRology.pdf

Georgakakos, A., Fleming, P., Dettinger, M., Peters-Lidard, C., Richmond, T., Reckhow, K., White, K., & Yates, D. (2014). NCA 2014: Chapter 3: Water resources. In *Climate change impacts in the United States: The third national climate assessment* (pp. 69–112). US Global Change Research Program. https://doi.org/10.7930/J0G44N6T

Graf, W. L. (1975). The impact of suburbanization on fluvial geomorphology. *Water Resources Research*, *11*(5), 690–692. https://doi.org/10.1029/WR011i005p00690

Haga, H., Matsumoto, Y., Matsutani, J., Fujita, M., Nishida, K., & Sakamoto, Y. (2005). Flow paths, rainfall properties, and antecedent soil moisture controlling lags to peak discharge in a granitic unchanneled catchment. *Water Resources Research*, *41*(12), 1–14. https://doi.org/10.1029/2005WR004236

Henderson, F. (1966). *Open channel flow*. Macmillan Publishing Co.

Hibbs, B. J., & Sharp, J. M. (2012). Hydrogeological impacts of urbanization. *Environmental and Engineering Geoscience*, *18*(1), 3–24. https://doi.org/10.2113/gseegeosci.18.1.3

Hirsch, R. M., & Archfield, S. A. (2015). Flood trends: Not higher but more often. *Nature Climate Change*, *5*(3), 198–199. https://doi.org/10.1038/nclimate2551

Historic Pittsburgh Maps (2021). *Pittsburgh historic maps*. University of Pittsburgh Library Digital Collections. https://www.arcgis.com/apps/View/index.html?appid=63f24d1466f24695bf9dfc5bf6828126

Hopkins, K. G., & Bain, D. J. (2018). Research note: Mapping spatial patterns in sewer age, material, and proximity to surface waterways to infer sewer leakage hotspots. *Landscape and Urban Planning*, *170*, 320–324. https://doi.org/10.1016/J.LANDURBPLAN.2017.04.011

Hopkins, K. G., Bain, D. J., & Copeland, E. M. (2013). Reconstruction of a century of landscape modification and hydrologic change in a small urban watershed in Pittsburgh, PA. *Landscape Ecology*, *29*(3), 413–424. https://doi.org/10.1007/s10980-013-9972-z

Hopkins, K. G., Bhaskar, A. S., Woznicki, S. A., & Fanelli, R. M. (2019). Changes in event-based streamflow magnitude and timing after suburban development with infiltration-based stormwater management. *Hydrological Processes*, *34*, 387–403. https://doi.org/10.1002/hyp.13593

Hopkins, K. G., Morse, N. B., Bain, D. J., Bettez, N. D., Grimm, N. B., Morse, J. L., Palta, M. M., Shuster, W. D., Bratt, A. R., & Suchy, A. K. (2015). Assessment of regional variation in streamflow responses to urbanization and the persistence of physiography. *Environmental Science and Technology*, *49*(5), 2724–2732. https://doi.org/10.1021/es505389y

Karpf, C., & Krebs, P. (2011). Quantification of groundwater infiltration and surface water inflows in urban sewer networks based on a multiple model approach. *Water Research*, *45*(10), 3129–3136. https://doi.org/10.1016/j.watres.2011.03.022

Kaushal, S. S., & Belt, K. T. (2012). The urban watershed continuum: Evolving spatial and temporal dimensions. *Urban Ecosystems*, *15*(2), 409–435. https://doi.org/10.1007/s11252-012-0226-7

Konrad, C. P., Booth, D. B., & Burges, S. J. (2005). Effects of urban development in the Puget lowland, Washington, on interannual streamflow patterns: Consequences for channel form and streambed disturbance. *Water Resources Research*, *41*(7), 1–15. https://doi.org/10.1029/2005WR004097

Kracht, O., Gresch, M., & Gujer, W. (2007). A stable isotope approach for the quantification of sewer infiltration. *Environmental Science and Technology*, *41*(16), 5839–5845. https://doi.org/10.1021/es062960c

Kracht, O., & Gujer, W. (2005). Quantification of infiltration into sewers based on time series of pollutant loads. *Water Science and Technology*, *52*(3), 209–218. https://doi.org/10.2166/wst.2005.0078

Kuliczkowska, E. (2017). Environmental and structural risk assessment of long operated vitrified clay sewers. *Environment Protection Engineering*, *44*(2), 53–67. https://doi.org/10.5277/epe170205

Kundzewicz, Z. W. (2008). Climate change impacts on the hydrological cycle. *Ecohydrology & Hydrobiology*, *8*(2–4), 195–203. https://doi.org/10.2478/V10104-009-0015-Y

Leopold, L. (1968). *Hydrology for urban land planning, A guidebook on the hydrologic effects of urban land use*. U.S. Department of the Interior.

Loehlein, M. D., Meeneghan, T. J., & Prevost, T. (2005). A continuous simulation approach for separate sewered areas. *Journal of Water Management Modeling*, *13*, 223–244. https://doi.org/10.14796/JWMM.R223-21

McMahon, G., Bales, J. D., Coles, J. F., Giddings, E. M. P., & Zappia, H. (2003). Use of stage data to characterize hydrologic conditions in an urbanizing environment. *Journal of the American Water Resources Association*, *39*(6), 1529–1546. https://doi.org/10.1111/j.1752-1688.2003.tb04437.x

Meierdiercks, K. L., Smith, J. A., Baeck, M. L., & Miller, A. J. (2010a). Heterogeneity of hydrologic response in urban watersheds. *Journal of the American Water Resources Association*, *46*(6), 1221–1237. https://doi.org/10.1111/j.1752-1688.2010.00487.x

Meierdiercks, K. L., Smith, J. A., Baeck, M. L., & Miller, A. J. (2010b). Analyses of urban drainage network structure and its impact on hydrologic response. *Journal of the American Water Resources Association*, *46*(5), 932–943. https://doi.org/10.1111/J.1752-1688.2010.00465.X

Merz, B., Vorogushyn, S., Uhlemann, S., Delgado, J., & Hundecha, Y. (2012). HESS Opinions: "More efforts and scientific rigour are needed to attribute trends in flood time series". *Hydrology and Earth System Sciences*, *16*(5), 1379–1387. https://doi.org/10.5194/hess-16-1379-2012

Miller, A. J., Welty, C., Duncan, J. M., Baeck, M. L., & Smith, J. A. (2021). Assessing urban rainfall-runoff response to stormwater management extent. *Hydrological Processes*, *35*(7), 1–11. https://doi.org/10.1002/hyp.14287

Napieralski, J., Keeling, R., Dziekan, M., Rhodes, C., Kelly, A., & Kobberstad, K. (2015). Urban stream deserts as a consequence of excess stream burial in urban watersheds. *Annals of the Association of American Geographers*, *105*(4), 649–664. https://doi.org/10.1080/00045608.2015.1050753

Napieralski, J. A., & Carvalhaes, T. (2016). Urban stream deserts: Mapping a legacy of urbanization in the United States. *Applied Geography*, *67*, 129–139. https://doi.org/10.1016/j.apgeog.2015.12.008

Napieralski, J. A., & Welsh, E. S. (2016). A century of stream burial in Michigan (USA) cities. *Journal of Maps*, *12*, 300–303. https://doi.org/10.1080/17445647.2016.1206040

Ntelekos, A. A., Smith, J. A., Baeck, M. L., Krajewski, W. F., Miller, A. J., & Goska, R. (2008). Extreme hydrometeorological events and the urban environment: Dissecting the 7 July 2004 thunderstorm over the Baltimore MD metropolitan region. *Water Resources Research*, *44*, 1–19. https://doi.org/10.1029/2007WR006346

Ogden, F. L., Raj Pradhan, N., Downer, C. W., & Zahner, J. A. (2011). Relative importance of impervious area, drainage density, width function, and subsurface storm drainage on flood runoff from an urbanized catchment. *Water Resources Research*, *47*(12), 1–12. https://doi.org/10.1029/2011WR010550

PAMAP Program Pennsylvania Department of Conservation and Natural Resources, Bureau of Topographic and Geologic Survey (2005). *PAMAP program – Land cover for Pennsylvania 2005*. http://www.pasda.psu.edu

Pangle, L. A., Diem, J. E., Milligan, R., Adams, E., & Murray, A. (2022). Contextualizing inflow and infiltration within the streamflow regime of urban watersheds. *Water Resources Research*, *58*, 1–19. https://doi.org/10.1029/2021wr030406

Pennino, M. J., McDonald, R. I., & Jaffe, P. R. (2016). Watershed-scale impacts of stormwater green infrastructure on hydrology, nutrient fluxes, and combined sewer overflows in the mid-Atlantic region. *Science of the Total Environment*, *565*, 1044–1053. https://doi.org/10.1016/j.scitotenv.2016.05.101

Poff, N. L. R., Allan, J. D., Bain, M. B., Karr, J. R., Prestegaard, K. L., Richter, B. D., Sparks, R. E., & Stromberg, J. C. (1997). The natural flow regime: A paradigm for river conservation and restoration. *BioScience*, *47*(11), 769–784. https://doi.org/10.2307/1313099

Roodsari, B. K., & Chandler, D. G. (2017). Distribution of surface imperviousness in small urban catchments predicts runoff peak flows and stream flashiness. *Hydrological Processes*, *31*(17), 2990–3002. https://doi.org/10.1002/hyp.11230

Roy, A. H., Dybas, A. L., Fritz, K. M., & Lubbers, H. R. (2015). Urbanization affects the extent and hydrologic permanence of headwater streams in a midwestern US metropolitan area. *Journal of the North American Benthological Society*, *28*(4), 911–928. https://doi.org/10.1899/08-178.1

Schreider, S. Y., Smith, D. I., & Jakeman, A. J. (2000). Climate change impacts on urban flooding. *Climatic Change*, *47*(1–2), 91–115. https://doi.org/10.1023/a:1005621523177

Schueler, T. R. (1994). The importance of imperviousness. *Watershed Protection Techniques*, *1*(3), 100–111.

Schueler, T. R., Fraley-Mcneal, L., & Cappiella, K. (2009). Is impervious cover still important? Review of recent research. *Journal of Hydrologic Engineering*, *14*(4), 309–315. https://doi.org/10.1061/ASCE1084-0699200914:4309

Sharp, J. M., Krothe, J. N., Mather, J., Garcia-Fresca, B., & Stewart, C. A. (2003). Effects of urbanization on groundwater systems. In *Earth science in the city: A reader* (pp. 257–278). American Geophysical Union.

Shuster, W. D., Bonta, J., Thurston, H., Warnemuende, E., & Smith, D. R. (2005). Impacts of impervious surface on watershed hydrology: A review. *Urban Water Journal*, *2*(4), 263–275. https://doi.org/10.1080/15730620500386529

Smith, B. K., Smith, J. A., Baeck, M. L., Villarini, G., & Wright, D. B. (2013). Spectrum of storm event hydrologic response in urban watersheds. *Water Resources Research*, *49*(5), 2649–2663. https://doi.org/10.1002/wrcr.20223

Smith, J. A., Baeck, M. L., Meierdiercks, K. L., Nelson, P. A., Miller, A. J., & Holland, E. J. (2005). Field studies of the storm event hydrologic response in an urbanizing watershed. *Water Resources Research*, *41*(10), 1–15. https://doi.org/10.1029/2004WR003712

Smith, J. A., Miller, A. J., Baeck, M. L., Nelson, P. A., Fisher, G. T., & Meierdiercks, K. L. (2005). Extraordinary flood response of a small urban watershed to short-duration. *Journal of Hydrometerology*, *6*, 599–617. https://doi.org/10.1175/JHM426.1

Soulsby, C., Birkel, C., & Tetzlaff, D. (2014). Assessing urbanization impacts on catchment travel times. *Geophysical Reserach Letters*, *41*, 442–448. https://doi.org/10.1002/2013GL058716

Trenberth, K. E. (1999). Conceptual framework for changes of extremes of the hydrological cycle with climate change. In T. R. Karl, N. Nicholls, & A. Ghazi (Eds.), *Weather and Climate Extremes* (pp. 327–339). Springer. https://doi.org/10.1007/978-94-015-9265-9_18

Valtanen, M., Sillanpää, N., & Setälä, H. (2014). Effects of land use intensity on stormwater runoff and its temporal occurrence in cold climates. *Hydrological Processes*, *28*(4), 2639–2650. https://doi.org/10.1002/hyp.9819

Walsh, C. J., Roy, A. H., Feminella, J. W., Cottingham, P. D., Groffman, P. M., & Morgan, R. P. (2005). The urban stream syndrome: Current knowledge and the search for a cure. *Journal of the North American Benthological Society*, *24*(3), 706–723. https://doi.org/10.1899/04-028.1

Weitzell, R., Kaushal, S., Lynch, L., Guinn, S., & Elmore, A. (2016). Extent of stream burial and relationships to watershed area, topography, and impervious surface area. *Water*, *8*(11), 538. https://doi.org/10.3390/w8110538

Wittenberg, H. (2003). Effects of season and man-made changes on baseflow and flow recession: Case studies. *Hydrological Processes*, *17*(11), 2113–2123. https://doi.org/10.1002/HYP.1324

Yang, L., Smith, J. A., Wright, D. B., Baeck, M. L., Villarini, G., Tian, F., & Hu, H. (2013). Urbanization and climate change: An examination of nonstationarities in urban flooding. *Journal of Hydrometeorology*, *14*(6), 1791–1809. https://doi.org/10.1175/JHM-D-12-095.1

SUPPORTING INFORMATION

Additional supporting information may be found in the online version of the article at the publisher's website.

How to cite this article: Forgrave, R., Elliott, E. M., & Bain, D. J. (2022). Event scale hydrograph responses highlight impacts of widespread stream burial and urban infrastructure failures. *Hydrological Processes*, *36*(5), e14584. https://doi.org/10.1002/hyp.14584

(Georgakakos et al., 2014). Due to this increased precipitation, both the overall magnitude of floods and their frequency are already increasing, and are predicted to increase further in the future (Hirsch & Archfield, 2015). Flooding in urban areas can damage buildings, roads, and other urban infrastructure (Schreider et al., 2000), as well as permanently alter ecosystems and habitat, jeopardizing the success of stream restoration projects (Bain et al., 2014).

Areas of urban land with predominantly buried surface waters have been called 'urban stream deserts' (Napieralski et al., 2015) and constitute over 11 000 km^2 of the contiguous US (Napieralski & Carvalhaes, 2016). Stream burial is more common in central portions of older North American cities, with extensive channel loss documented in Baltimore, MD (Elmore & Kaushal, 2008; Weitzell et al., 2016), Washington, DC (Weitzell et al., 2016), Cincinnati (Roy et al., 2015), Detroit, MI (Napieralski & Welsh, 2016), and Pittsburgh, PA (Hopkins & Bain, 2018). In these cities, headwaters are often preferentially buried because of their small size and spatial prevalence (Leopold, 1968).

Stream burial decreases hydrologic residence time because artificial channels and pipes are smoother and straighter than natural channels so water passes through more quickly (Henderson, 1966; Kaushal & Belt, 2012). Decreased residence time in headwater channels can result in higher flows downstream (Ogden et al., 2011), as water from more distant parts of the catchment reach the watershed outlet at the same time as nearby tributaries, Additionally, relocating stream channels to pipes complicates the connections between surface water, hyporheic zone, and riparian areas (Broadhead et al., 2013; Hopkins & Bain, 2018). Burying streams can completely separate surface water from hyporheic and soil flowpaths and prevent exchange of water. Older pipes are more likely to leak, leading to spatially heterogeneous hot-spots of infiltration and exfiltration throughout the buried drainage network (Bhaskar & Welty, 2012). The dense network of subsurface pipe conveyance created by widespread stream burial has been called 'urban karst' (Bonneau et al., 2017; Hibbs & Sharp, 2012; Kaushal & Belt, 2012). Buried pipes are often surrounded by high permeability sand and gravel that acts as a preferential flowpath for drainage of groundwater in the basin (Soulsby et al., 2014) and promote lateral movement and interactions with sewer and drinking water pipes (Sharp et al., 2003). Runoff models like SWMM do not account for pipe leakage or the preferential flowpaths around them (Bonneau et al., 2017) so the contributions from these urban water subsidies are seldom included in event studies (Bhaskar & Welty, 2012).

Watershed response to storm events can be complicated because stream discharge is a mixture of precipitation inputs and water stored in the watershed. Overland flow across impervious surfaces is the dominant transport mechanism for both water and pollutants in urban streams (Buda & DeWalle, 2009), but storm flow still contains a considerable proportion of pre-event water, ranging 20%–90%, due to groundwater travelling through urban karst (Meierdiercks et al., 2010b). Delineating the relative contribution of event and pre-event waters is challenging and there are several methods, using tracers, graphical approaches, or digital filters (Blume et al., 2007). 'Event flow' can be categorized as rainfall from a particular event, or the results of a rapid increase in hydraulic head that causes a fast release of groundwater discharge and thus a mixture of old and new water (Wittenberg, 2003). Dingman (2002) defined event flow as water volume attributable to a single event, thus, event flow includes surface runoff, interflow, sewer overflows, and fast groundwater response as a direct reaction to rainfall inputs.

Flow separation is more complex in urban systems due to contributions from combined and sanitary sewer overflows to stream discharge. Combined sewers are single pipe systems with both storm water and sanitary sewage combined in the same pipes. During flows that exceed pipe capacity, combined sewer pipe systems are designed to overflow into surface water. Separated sanitary sewers also have overflows in the case of excess pressure, which can occur when pipe capacity is exceeded from high infiltration into sewers during storm events (EPA, 2004; Pangle et al., 2022). For our purposes, both types of sewer overflows are also considered event flow because an individual overflow event is directly related to a given storm event.

To clarify patterns in buried stream event responses, we investigate the following questions in this study: How does widespread headwater stream burial affect the hydrograph response to precipitation inputs? Are there seasonal trends in the rainfall-runoff relationship? Do the thresholds of change in this relationship reveal connections among the various networks of subsurface urban infrastructure?

2 | DATA AND METHODS

2.1 | Study site

The Nine Mile Run watershed drains 15.7 km^2 of eastern Pittsburgh, PA and surrounding suburban communities. The watershed is 38% impervious surfaces and predominantly urban land cover (66%); the remainder is 18% forested, 10% grassy field, and 5% barren land (PAMAP Program Land Cover for Pennsylvania, 2005) (Figure 1b). Half of the watershed is served by combined sewers and half by separated storm and sanitary sewer networks (Figure 1c). About 60% of this sewer network in Nine Mile Run is made of vitrified clay pipe (Joe Fedor, personal communication), which commonly fails along pipe joins (Kuliczkowska, 2017). A majority of the headwaters of Nine Mile Run were buried in the 1920s (Historic Pittsburgh Maps, 2021) during a time of rapid residential development (Hopkins et al., 2013). These buried channels were often deliberately located in the same pipes as the storm sewer network (Hopkins & Bain, 2018). Today, almost all headwater channels in the Nine Mile Run watershed are buried (3 Rivers 2nd Nature, 2006), with only the most downstream portion in a restored surface channel (Figure 1b). This multi-million dollar stream restoration project was completed in 2006 and aimed to restore the main stem of Nine Mile Run, prevent erosion and flooding by connecting the stream to the adjacent floodplain wetlands, and support the recovery of instream biotic communities (Bain et al., 2014). While there were water quality and ecological improvements following restoration, this effort did not address the effects of headwater stream burial on downstream flooding.

2.2 | Data collection

We measured Nine Mile Run discharge with a HOBO pressure transducer (Onset Computer Corporation, Bourne, MA) in a stilling well installed in 2014, 300 m downstream of the culvert where the above ground portion of Nine Mile Run emerges (Figure 1). The rating curve for this pressure transducer was created with 12 paired stage-discharge measurements collected from 2014–2015 at a variety of flow conditions. The gauged reach is a concrete, trapezoidal channel, so the stage-discharge relations should remain relatively stable over time. The highest storm flow we could safely measure was 1.02 m^3/s, resulting in higher uncertainty in the stage-discharge relationship at flows above this threshold (Figure S1). The coefficient values for the rating curve were determined with an iterative non-linear least-squares regression method in R, and each have their own associated error. This uncertainty in coefficients was used to calculate a range of potential discharge values for any given stage (Figure S1). The distribution of discharge from the pressure transducer record collected for this study was comparable to the distribution of discharge data from a USGS gage (03085049, active 2006–2009) that was installed farther downstream (Kolmogorov–Smirnov test, $p < 0.0001$, Figure S2). The upstream discharge measured with the pressure transducer was often larger than the downstream discharge measured with the USGS gage due to sewer infiltration (Divers, unpublished data).

The watershed metrics calculated for this study only considered the portion of the watershed that drained directly to the gauged reach rather than the entirety of Nine Mile Run This headwater subwatershed above the pressure transducer drained a land area of 8.2 km^2, is 81% urban land use, and has 98% of all channel length buried, so it was an ideal location for investigating the effects of channel burial on storm event responses.

The buried subwatershed is served by separated storm and sanitary sewer networks. There were several gaps in the discharge record due to equipment malfunction of the pressure transducer, barometric correction station, or data shuttle, as well as the clogging of the stilling well access following a large flow event (Table 1, Figure 2). These data

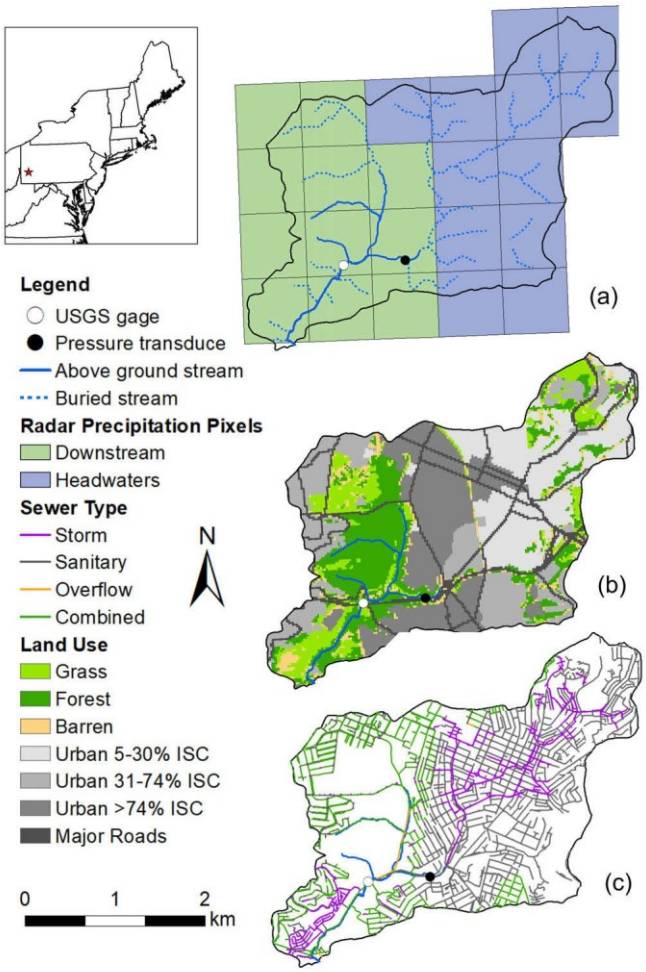

FIGURE 1 Maps of the Nine Mile Run watershed showing: (a) buried streams (dotted lines) and surface streams (solid lines) along with radar precipitation pixels designated as headwater or downstream based on the location of the discharge sensor (black dot). USGS gage installed from 2006–2009 is shown in the white dot. Map (b) shows the currently visible surface stream channels and land use from PAMAP Program Land Cover for Pennsylvania 2005. Map (c) shows the sanitary and combined sewer networks of the Nine Nile Run watershed

TABLE 1 Summary of discharge data record with data gaps and storm events by year

Year	Percentage of days missing from flow record	Number of storm events
2014	45%	47
2015	9%	81
2016	48%	36
2017	26%	79
2018	38%	68
2019	0%	126
2020	12%	88

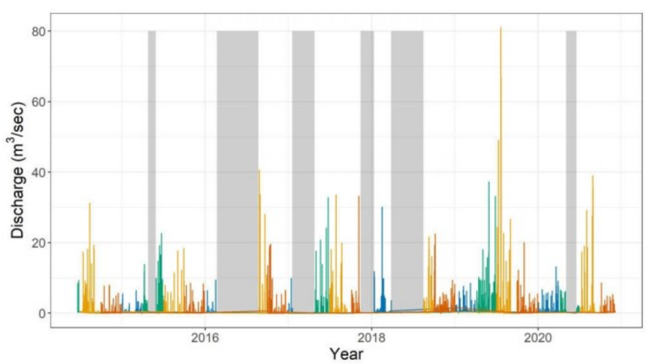

FIGURE 2 15-minute flow data time series for the entire study period (2014–2020). Gaps in data are highlighted by grey shading. Line colour designates seasons with spring in green, summer in yellow, fall in red, and winter in blue. 2019 stands out as an extremely wet with year with four of the overall 10 largest events gaps occur in all seasons but are slightly more common in spring, potentially biasing comparison of events across seasons.

Watershed precipitation data was obtained from NEXRAD radar calibrated by a network of 33 rain gages across Allegheny County (3 Rivers Wet Weather, 2021). This data included rainfall depths for every 1 km^2 grid cell in Allegheny County at 15-min intervals (Loehlein et al., 2005). For this analysis, rainfall from the 12 pixels that overlay the buried watershed (Figure 1a) was averaged to calculate a precipitation depth for each 15-min interval.

2.3 | Storm selection

The Nine Mile Run discharge data and radar precipitation data were joined into a single dataset by matching timestamp to create a 7-year record (2014–2020). We used the BaseflowSeparation function within the *EcoHydRology* R package, to separate the discharge record into 'quickflow' and 'baseflow' components using a recursive digital filter (Fuka et al., 2018), with a filter parameter of 0.99 and three passes. This filter parameter is recommended over the traditional 0.95 or 0.925 for sub-hourly time steps (Duncan, 2019; Hopkins et al., 2019) and was validated by visually inspecting hydrographs. Storm events were selected from the discharge record based on three criteria: (1) discharge greater than the threshold of 0.8 m^3/s, (2) event quickflow (Q_t) greater than 0.5 m^3/s, and (3) a discharge slope greater than a threshold slope (S_t) of 0.01 m^3/s calculated as discharge minus a 4-h leading (t_{i+4}) and 2-h lagging minimum discharge (t_{i-2}) (adapted from Hopkins et al., 2019). The thresholds were chosen to ensure that each storm was above baseflow conditions, which vary widely throughout the year. This selection process resulted in a set of 448 discharge events. Each of these identified hydrograph events were then matched with the most recent precipitation event up to 3 h before the corresponding hydrograph event. We identified precipitation events as periods of time when precipitation was greater than 0 mm, where a break in precipitation greater than 2 h was considered a separate precipitation event, resulting in a total of 1309 distinct precipitation events. There were many more precipitation events than flow events because there are no gaps in the precipitation data, and extremely small precipitation events did not produce a detectable a flow event.

In several cases (n = 84), multiple distinct discharge peaks were classified as the same event because the stream did not return to baseflow conditions before the next precipitation event created a discharge response. These were manually separated at each streamflow minima. In sum, a total of 525 matching discharge and precipitation events were used in the following analyses. For seasonal analyses, spring is March 20th–June 19th, summer is June 20th–September 21st, fall is September 22nd–December 20th, and winter is December 21st–March 19th.

2.4 | Event metrics and statistics

For each paired precipitation-discharge event, the precipitation metrics calculated included: total event precipitation depth (mm), precipitation event duration (h), precipitation intensity (mm/h), and 5-day total antecedent precipitation depth (mm). For all precipitation metrics, only the buried watershed area above the pressure transducer was considered. We chose 5-day antecedent precipitation as a measure of antecedent conditions because it is more directly comparable to flow metrics than measurements of soil moisture (Smith et al., 2013). The hydrologic response variables were hydrograph peak duration (h), maximum discharge (m^3/s), runoff yield (total runoff volume converted to a depth by dividing by watershed area) (mm), and the hydrograph rise time (hours from start of hydrograph event to peak of discharge).

To evaluate the relationships between precipitation and discharge events, we calculated runoff ratio and lag time. Runoff ratio, also called runoff coefficient, is a unitless volume ratio of event rainfall to either total flow volume or quickflow volume (Blume et al., 2007). Runoff ratio can be calculated in an annual or event basis. Since this paper focuses on events, we calculate runoff ratio as total quickflow divided by total event rainfall for each event. Lag time is the amount of time between the precipitation event and hydrograph event. It is often calculated as the hours between the centroid of precipitation and the maximum discharge (Smith et al., 2013), but for some events with very fast watershed responses and extended precipitation, the maximum flow occurred before the centroid of precipitation which would result in a negative lag time, so we chose to use the time between the start of precipitation and start of the hydrograph rise.

We assessed correlations between maximum discharge, runoff yield, and event precipitation using simple linear regression performed in R. Except for runoff ratio, all precipitation and discharge response variables were log transformed for linear regressions. Runoff ratio is approximately normal without transformation. While log transformed data are not statistically normal, they do follow an approximate Gaussian shape, with the exception of streamflow rise time (Figure 3). Rise time is limited by the 15-min data collection interval, so anything faster than 15-min will appear in the data as a 0-min rise time, and thus be removed from log-transformed data. Seasonal variation in both the precipitation input and watershed response metrics listed above were assessed with ANOVAs and Tukey's post-hoc tests performed in R.

3 | RESULTS

3.1 | Precipitation events and hydrologic responses

Over the full study period from 2014–2020, there were 525 distinct storm events that met the criteria defined above (Figure 2, Table 2). 2019 was the wettest year during the study period with a total of 1328 mm of precip from 130 storm events and was also the only year in the record with no data gaps (Table 1). Total event precipitation depth ranged from 0.24 to 181.7 mm, and event duration spanned from 0.25 to 63.5 h. Precipitation event intensity ranged from 0.2 to 45.4 mm/h. The 5-day antecedent precipitation depth prior to event onset ranged from 0.0 to 87.5 mm. In terms of event responses,

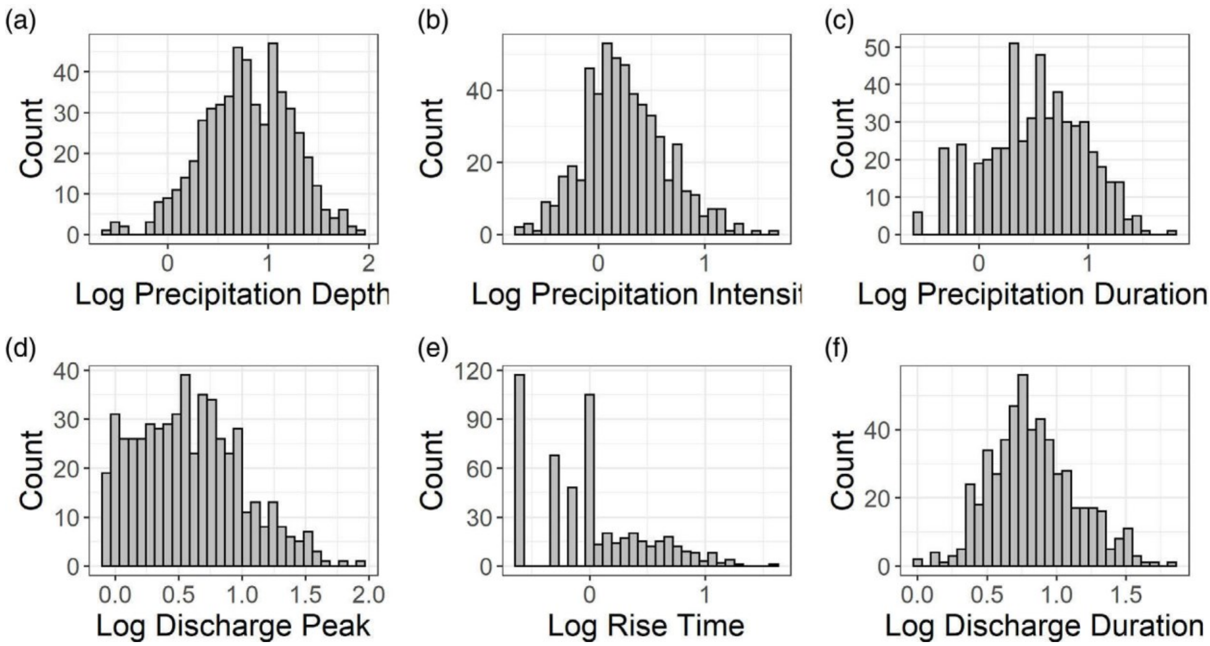

FIGURE 3 Histograms of log transformed data: (a) precipitation depth, (b) precipitation intensity, (c) precipitation duration, (d) peak discharge, (e) hydrograph rise time, and (f) discharge duration. All distributions except rise time are approximately normal, though they are all statistically different from normal due to the influence of a few outliers (Shapiro–Wilk test, precipitation depth: $p = 0.0036$, precipitation intensity: $p = 0.0027$, precipitation duration: $p = 0.0019$, discharge peak: $p < 0.0001$, rise time: $p =$ NA, discharge duration: $p = 0.0008$)

TABLE 2 Summary statistics of event metrics

	Mean	Median	Minimum	Maximum
Precipitation metrics				
Total event precipitation (mm)	10.22	6.32	0.24	181.67
Precipitation duration (h)	5.62	3.75	0.25	63.50
Precipitation intensity (mm/h)	2.76	1.64	0.18	45.38
5-day antecedent precip (mm)	16.75	13.23	0.00	87.47
Hydrograph response metrics				
Peak discharge (m^3/s)	6.13	3.65	0.81	81.05
Hydrograph event duration (h)	9.02	6.25	1.00	81.50
Runoff yield (mm)	5.02	2.49	0.24	124.56
Rise time (h)	1.92	0.75	0.00	39.50
Combined metrics				
Lag time (peak starts) (h)	2.11	1.75	0.00	13.00
Runoff ratio	0.46	0.42	0.10	3.14

discharge events spanned between 1.0 and 81.5 h in duration. Lag times between the start of the precipitation event and the start of the discharge event ranged from 0.0 to 13.0 h with a median of 1.8 h. Hydrograph rise time ranged from 0.0 to 39.5 h with median of 0.75 h. Measurement of response time is fundamentally limited by the data collection interval (15 min). There were 24 events where the rise time from the start of hydrograph rise to its peak was 15 min or less, meaning that the entire hydrograph rise occurred between data collection points. These extremely fast storms have hydrograph rise ranging from 14.1 to 40.6 m^3/s in that 15-min interval. Peak discharge ranged from 0.81 to 81.1 m^3/s. This highest flow is 400x the average baseflow condition of 0.2 m^3/s. For these extremely high peaks, the error of the coefficients of the stage-discharge curve means the 81.1 m^3/s peak flow could be anywhere between 55.3 and 110.1 m^3/s.

3.2 | Relationships among the precipitation and streamflow metrics

In general, longer precipitation events led to longer flow events ($R^2 = 0.605$, $p < 0.001$). A higher precipitation depth led to both higher peak streamflow ($R^2 = 0.523$, $p < 0.001$, Figure 4a) and a larger runoff yield ($R^2 = 0.889$, $p < 0.001$, Figure 4d). Although higher precipitation intensity resulted in higher peak streamflow ($R^2 = 0.526$, $p < 0.001$, Figure 4b), the relationship between precipitation intensity and runoff yield was weak ($R^2 = 0.142$, $p < 0.001$, Figure 4e). These relationships are affected by the presence of a few storms with very high flows, or very low precipitation, but are not considered outliers (Rosner's test in the *EnvStats* R package) and are thus not excluded from the analysis. Neither peak streamflow nor runoff yield were correlated with 5-day antecedent precipitation (Figure 4c,f) and thus indicated that pre-event water plays a negligible role in determining event response.

3.3 | Seasonal variation in watershed response

Throughout the study period, summer had the highest total number of storms ($n = 167$), followed by fall ($n = 137$), spring ($n = 123$), whereas winter had the fewest storms ($n = 99$). However, there were several month-long gaps in the flow data that could affect these numbers. While days without data occurred in all seasons, the majority of them (56%) occurred in spring and fewest in fall (5%) (Figure 2), so spring storms will be slightly underrepresented in this analysis compared to their actual frequency. To illustrate this point, if we consider only years where <15% of the flow data is missing (2015, 2019, and 2020), the greatest number of storms was in the spring or summer, followed by winter or fall.

The average event precipitation depth for each season was within 3.2 mm of each other (winter = 10.4 mm, spring = 8.3 mm, summer = 9.4 mm, and fall = 11.5 mm), and there was a significant difference between precipitation depth in both spring and summer (drier) and fall (wetter) seasons (Tukey's test, $p = 0.02$ for spring–fall, $p = 0.04$ for summer–fall, Figure 5a). These seasonal differences in precipitation were more apparent in precipitation event duration. Pittsburgh has a humid climate that experiences convective thunderstorms in the late spring and summer. These thunderstorms storms deliver similar amounts of precipitation in a shorter time interval, averaging 3.3 and 4.2 h for spring and summer, relative to 7.6 and 8.3 h for fall and winter (ANOVA, $p < 0.001$, Table 3, Figure 5b). The shorter duration summer and spring precipitation events lead to significant differences in precipitation intensities with an average intensity of 4.5, 2.6, 1.9, and 1.2 mm/h for summer, spring, fall, and winter, respectively (ANOVA, $p < 0.001$, Table 3, Figure 5c).

This intense precipitation in summer and spring led to rapid and high discharge responses. The average summer hydrograph peak (9.2 m^3/s) is nearly twice as large as in fall (4.6 m^3/s) and winter (3.8 m^3/s). Summer discharge peaks were significantly higher compared to fall and winter (Tukey's test, $p < 0.001$ for summer–winter, $p < 0.001$ for summer–fall) and spring was significantly higher than winter (Tukey's test, $p = 0.005$, Figure 5f). Spring and summer

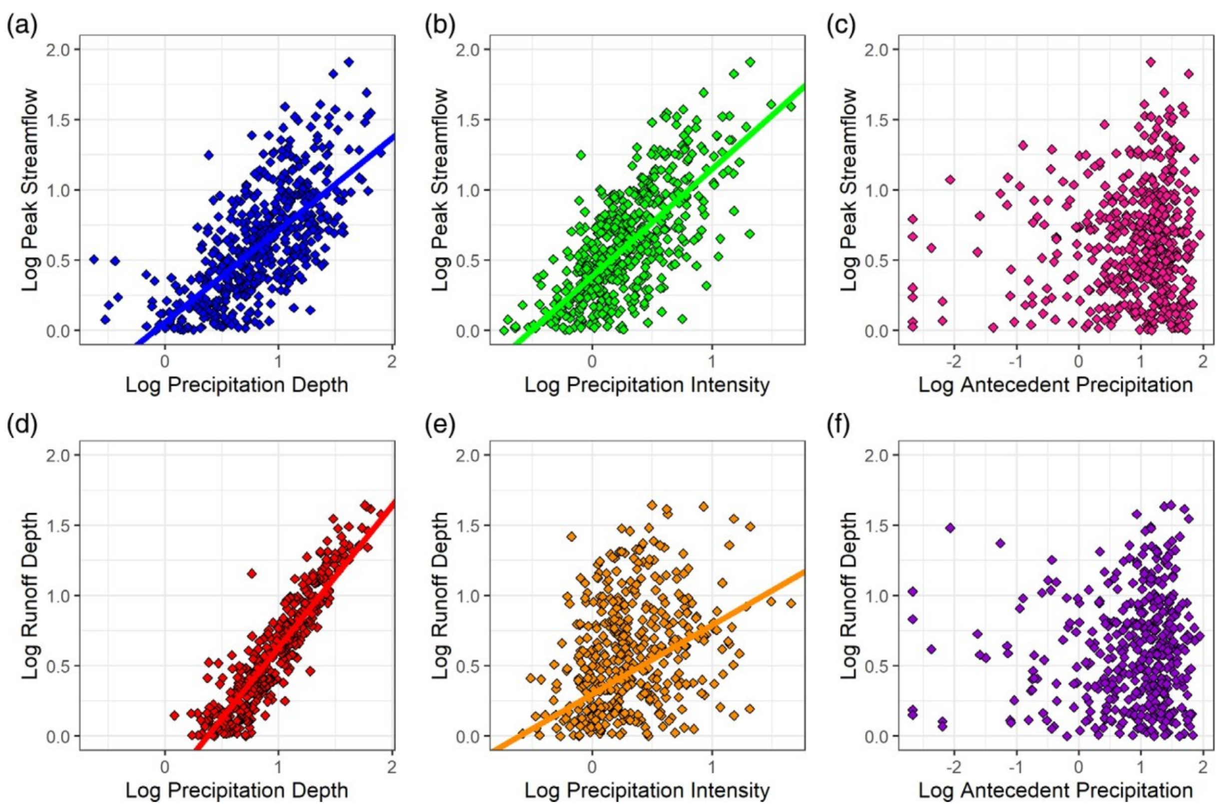

FIGURE 4 Linear regressions showing relationships among log-transformed precipitation and hydrograph response variables. Each data point is a storm event, and the line shows the linear regression.

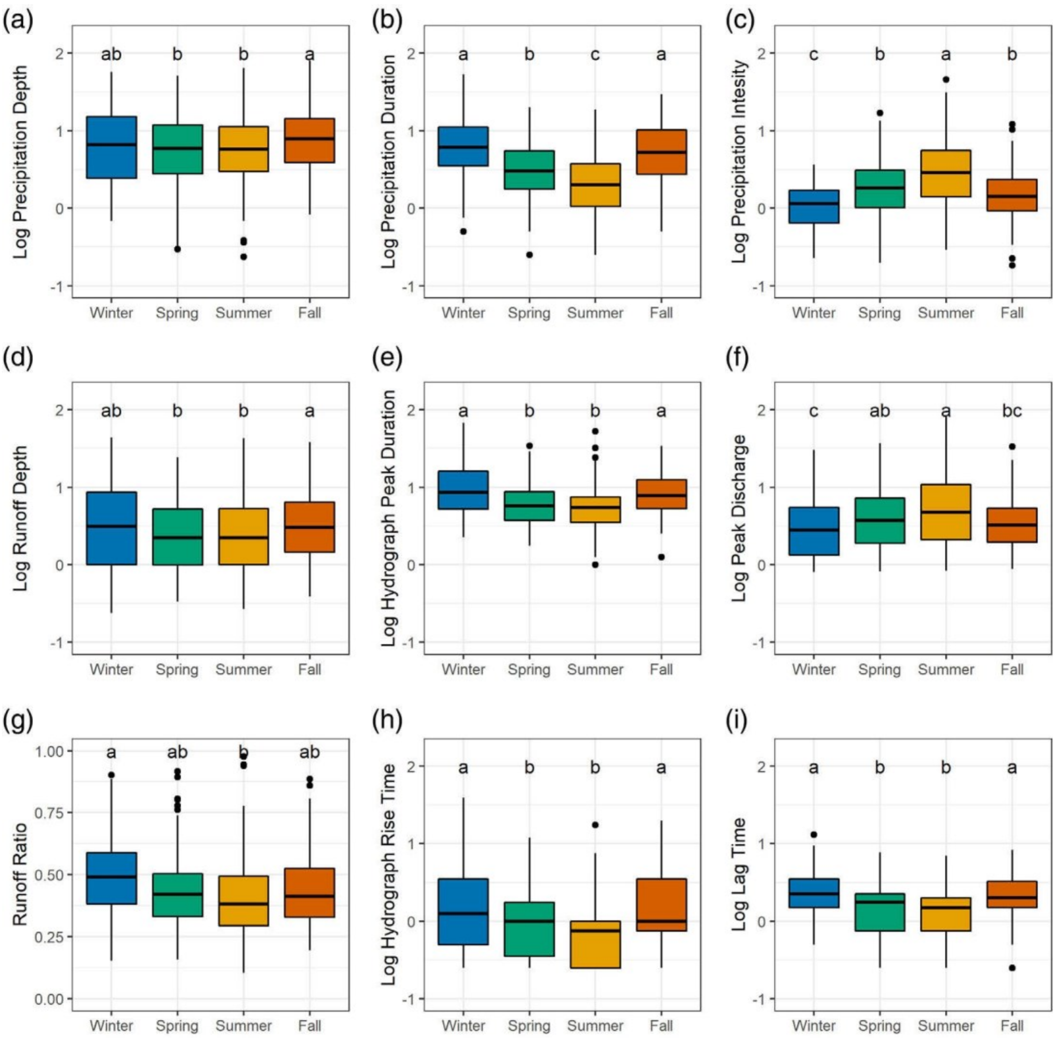

FIGURE 5 Seasonal differences in event metrics: (a) event precipitation, (b) precipitation intensity, (c) precipitation duration, (d) runoff depth, (e) peak discharge, (f) hydrograph peak duration, (g) runoff ratio, (h) hydrograph response time, and (i) lag time. All metrics except runoff ratio are log-transformed. Letters indicate significant differences from Tukey's post-hoc comparison. Events with runoff ratios greater than 1 are not shown

TABLE 3 Average event metrics separated by season

Event metric	Winter	Spring	Summer	Fall
Event precipitation (mm)	10.37	8.24	10.44	11.46
Precipitation intensity (mm/h)	1.24	2.60	4.48	1.92
Precipitation duration (h)	8.26	4.17	3.39	7.63
Runoff depth (mm)	5.97	3.69	5.19	5.34
Flow peak (m^3/s)	3.80	5.84	9.20	4.59
Flow peak duration (h)	12.38	7.43	7.07	10.48
Runoff ratio	0.55	0.47	0.48	0.46
Rise time (h)	3.04	1.28	1.10	2.61
Lag time (h)	2.73	1.76	1.61	2.51

discharge events were both of significantly lower duration (Tukey's test, $p < 0.001$ relative to summer–winter, summer–fall and spring–winter, $p = 0.001$ for spring–fall, Figure 5e). This reflects the fact that spring and summer storms tend to be a single discharge peak followed by a recession, whereas longer-duration storms in fall and winter often have multiple peaks in response to individual pulses of precipitation inputs, leading to an overall longer time above baseflow conditions. Discharge rose more quickly in summer and spring, 1.1 and 1.3 h, respectively, compared to 2.6 h for fall and 3.0 h for winter (Tukey's test, $p < 0.001$ for summer-winter and summer-fall, $p = 0.003$ for spring-winter, and $p = 0.002$ for spring-fall, Figure 5h). The lag time between precipitation and flow events also followed this same pattern of shorter in summer and spring than fall and winter (Tukey's test, $p < 0.001$ for summer-winter, summer-fall, spring-winter, and spring-fall, Figure 5i).

3.4 | Runoff ratios

The average event-specific runoff ratio across the full dataset was 0.48 ± 0.27. The average value for winter (0.50 ± 0.17) was slightly higher than the other seasons (spring = 0.47 ± 0.23, summer = 0.48 ± 0.37, fall = 0.46 ± 0.23), but this difference was not significant (ANOVA, $p = 0.22$, Figure 5g). The high standard deviation shows considerable variation in runoff ratios among events. However, almost none of the observed variability in runoff ratios can be explained by log-transformed event precipitation (linear regression, $R^2 = 0.003$, $p = 0.003$), precipitation intensity ($R^2 = 0.002$, $p = 0.13$), or pre-event discharge ($R^2 = 0.056$, $p < 0.001$).

3.5 | Time lags between precipitation and streamflow

Across all events, the lag time between the start of the precipitation and start of the hydrograph event was an average of 2.1 h, but it ranged from less than 15 min up to 13 h. There were 70 events with a lag time of 30 min or less, showing the Nine Mile Run system is extremely reactive to rainfall. One example of these storms with a 15-min lag time is shown in Figure 6.

4 | DISCUSSION

4.1 | Buried streams are the flashiest urban streams

Although urban streams are often described as 'flashy', characterized by faster hydrograph rise and fall than rural reference streams (Walsh et al., 2005), the widespread channel burial in Nine Mile Run makes it respond faster and with a larger peak discharge per square kilometre of drainage area than most other urban streams (Table 4). Throughout the literature, hydrograph 'flashiness' has had several definitions

TABLE 4 Summary of watershed flashiness in this study and other urban streams in the literature

Metric defining 'flashiness'	This study (buried stream)	Other urban streams
Fast watershed response time/ lag time	Average of 79 min	Average of 102 min (Smith et al., 2013)
Short hydrograph rise time	Average of 45 min	Less than 1 h (Smith et al., 2013)
Frequent high flow events	Average of 16.7 events/year over 1 $m^3/s/km^2$	12 events/year over 1 $m^3/s/km^2$ (Smith, Miller, et al., 2005)
Short duration of elevated flow conditions	24% of the record over mean flow	30% of total time above mean flow (Konrad et al., 2005)

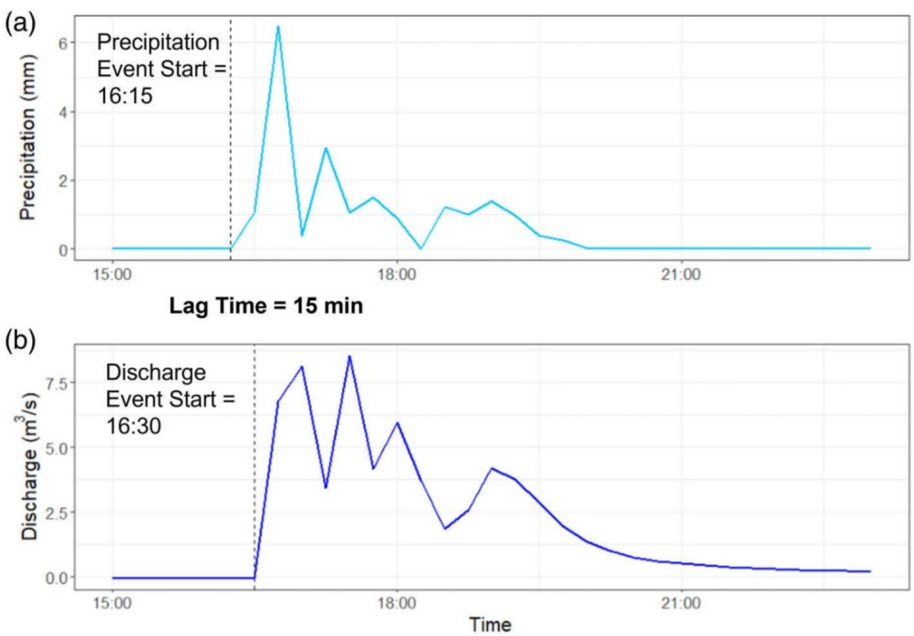

FIGURE 6 Precipitation and discharge time series for one example storm to illustrate the short lag time between the start of the precipitation event and the start of the rise in discharge. This event is from 15:00-23:00 on July 7, 2017

based on fast watershed response time (Smith et al., 2013), high rate of change in hydrograph on both rising and falling limbs (McMahon et al., 2003; Poff et al., 1997), the short duration of elevated flow conditions (Konrad et al., 2005; McMahon et al., 2003), or high frequency of events over a specific threshold (Smith et al., 2013; Smith, Miller, et al., 2005).

In the context of flashiness reported for urban streams, the largest 50 events recorded in Dead Run (30% impervious) in Baltimore from January 2000–December 2009 had an average watershed response time, also known as lag time, of 102 min from the time of the rainfall centroid to the peak discharge (Smith et al., 2013). In contrast, in Nine Mile Run (38% impervious), the largest 50 events have an average lag time of 41 min from centroid of precipitation to flow peak (Figure 6). This number is complicated by the fact that nine of these storms have negative lag times using this approach, where the peak discharge occurs before the bulk of precipitation has occurred, due to an extremely fast hydrograph rise. For this reason, we chose to use the time between precipitation start and start of hydrograph rise as the lag time for all events. Using this approach, the watershed response time of the largest 50 storms events averages 79 min, still 22% faster than Dead Run. The short lag times in urban watersheds are due to impervious surfaces that prevent infiltration and engineered drainage systems that efficiently route runoff to streams. This drainage efficiency means that rain falling in the headwater can reach the watershed outlet almost as fast as rain falling adjacent to the channel. In general, event lag times scale with the percent impervious cover (Meierdiercks et al., 2010b). However, as demonstrated in this study, stream burial further accelerates the short lag times of urban streams due to the integration of surface, soil, and pipe flowpaths that routes all water in pipe networks engineered to conduct water as fast as possible. As a result, any precipitation in the Nine Mile Run watershed reaches the stream via the fastest route possible soon after the storm begins.

In contrast to lag times that include both the time for rain to become runoff and travel times through watershed flowpaths, hydrograph rise time—the amount of time between when stream discharge starts to rise and when it reaches peak discharge—only reflects runoff travel times. The median hydrograph rise time in Nine Mile Run for all events was 45 min, but there are 28 events with a rise time of 15 min or less. This rise time is comparable to urban watersheds in the Baltimore area where six watersheds have hydrograph rise times of less than an hour and three of them are less than 15 min, (Smith et al., 2013). One notable difference is that the Baltimore study only quantifies the 50 largest storm events in a 10-year period for each watershed, whereas we characterize the median rise time for this study based on all events in a 6.5-year period. In Baltimore, rise times were not related to land use, but time period of urban development and presence of stormwater detention infrastructure (Smith et al., 2013). In contrast, buried streams have no stormwater detention facilities and instead conduct all stormwater to the stream as fast as possible, explaining the extremely fast rise times. A study of urban and suburban watersheds in New York state found a decrease in rise times with urbanization that is closer to the watershed outlet as opposed to farther away in the headwaters (Roodsari & Chandler, 2017) but this spatial organization of landscape impacts is less relevant when the stream is fully-buried, because all flowpaths are artificial drainages and travel times from the headwaters to the outlet are extremely fast.

The rapid hydrograph rise time in urban streams translates to a shorter overall time in elevated flow conditions compared to rural streams (McMahon et al., 2003). In Nine Mile Run, there were 58 events where the entire hydrograph rise and recession occur in less than 3 h. These quick events had some large flows: one event rose up to 18 m^3/s and back down to 0.3 m^3/s in less than 3 h. The overall impact of fast hydrograph changes can be quantified by comparing the percentage of time that a stream exceeds its mean streamflow over long time periods (Konrad et al., 2005). For example, urban streams in the Puget Sound region of Washington State had less than 30% of the total time above mean flows (Konrad et al., 2005). During the study period, Nine Mile Run is similar with flows exceeding the mean discharge only 24% of the total record.

The frequency of rapid storm response is also indicative of stream flashiness. Moores Run in Baltimore (9.1 km^2) has been reported as one of the flashiest streams in the contiguous US based on a 10-year dataset with an average of 12 events per year when discharge exceeded 1 $m^3/s/km^2$ (Smith, Miller, et al., 2005). These frequent high flows are attributed to high urbanization (82% urban land use), stream burial in the upper watershed, efficient concentration of runoff in the storm drain network, and a lack of stormwater detention structures (Smith et al., 2013; Smith, Miller, et al., 2005). The Nine Mile Run buried subwatershed, which is a comparable size (8.2 km^2) and urbanization (81% urban land use), had 117 total events exceeding this same discharge threshold of 1 $m^3/s/km^2$ threshold in 6.5 years of data with an average of 16.7 events per year. The frequency of fast storm responses in these two extremely impacted urban watersheds supports the role of stream burial in generating flashy storm response. Most discussions of flashy urban streams have focused on urban watersheds where total imperviousness or connected imperviousness is a primary driver of fast storm responses, whereas Hopkins et al. (2015) emphasized the importance of regional physiographic characteristics in determining the relationship between urban development and high flows. Catchments with shallower slopes, higher soil permeability, and more lakes, such as Boston, MA; Detroit, MI; Portland, OR; and St. Paul, MN can buffer the impacts of urbanization and generally have lower peak flows compared to cities in areas with higher slopes or less permeable soils including Pittsburgh, PA; Atlanta, GA; and Raleigh, NC (Hopkins et al., 2015). Conversely, Roodsari and Chandler (2017) found that when comparing watersheds within a single region, catchment morphology, hydraulics, topography, and soils were less correlated with runoff peak flows and stream flashiness than the percentage of artificial pathways in the watershed. This study supports both of these previous studies and demonstrates that in addition to regional physiographic characteristics, the type of urban development also impacts event responses. The Nine Mile Run subwatershed has steep slopes, impermeable soils, but also is composed of 98% buried channels. This dominance of stream burial creates a system where streamflow responses are higher, faster, and more frequent than other urban watersheds of comparable size, imperviousness, and underlying geology.

4.2 | Dominance of convective summer thunderstorms in climate-driven flooding

Throughout the study period, convective summer thunderstorms dominated the overall watershed response. These storms are intense localized storms triggered by the vertical movement of heat and moisture and characterized by heavy rain, thunder, lighting, strong winds, and sudden changes in temperature (Smith, Baeck, et al., 2005; Smith, Miller, et al., 2005). Intense summer storms dominated overall storm response trends because of the high discharge peaks, short duration, and small spatial area (Figure 5b,c), and also because summer had, on average, more storm events than other seasons. While this finding in itself is not new (Valtanen et al., 2014; Yang et al., 2013), it is important because warm season thunderstorms are the primary mechanism of flashy floods in urban environments (Ntelekos et al., 2008; Smith, Baeck, et al., 2005; Smith, Miller, et al., 2005). These summer rainfall events are predicted to become more intense in next decades as warmer air temperatures lead to a higher frequency of intense storms (Drum et al., 2017; Hirsch & Archfield, 2015). Urban areas can even increase likelihood of thunderstorms because the urban heat island effect can create convergence zones above and downwind of the urban area, as well as the increased concentration of aerosols from emissions can increase rainfall and streamflow in urban streams (Bornstein & Lin, 2000; Ntelekos et al., 2008). This climatic pressure will be even more apparent in watersheds with buried streams because the pipes that contain buried streams were built to accommodate the stream flow of 100 years ago, whereas increased runoff from development and climate change leads to stream flows that exceed pipe capacity. Urban stream deserts with no surface stream channels due to complete burial, which comprise the 6% of all urban land across the continental U.S., are more likely to flood, potentially affecting up to 73 million people (Napieralski & Carvalhaes, 2016).

4.3 | Runoff ratios reflect water subsidies from failing urban infrastructure

Runoff ratios describe how landscapes transform rainfall inputs into runoff that contributes to streamflow (Blume et al., 2007) where high values can indicate higher risk of surface floods. The average annual runoff ratio is 0.46 for Nine Mile Run and reveals that for a typical event, half of the event rainfall becomes runoff in the stream. The other half infiltrates into soil, groundwater, or buried pipe infrastructure, where it is released back into the stream after the event or lost to evapotranspiration. In the case of pipe infiltration, water can also be transported to other watersheds via sanitary sewer networks. Despite seasonal variation in precipitation amounts and hydrograph responses, event runoff ratios are consistent throughout the year (Figure 5g), suggesting that this metric reflects the effects of urban infrastructure on flow routing rather than any hydroclimate pattern.

Runoff ratios are usually related to antecedent rainfall (Haga et al., 2005; Smith, Baeck, et al., 2005; Smith, Miller, et al., 2005). For example, when a watershed is more saturated from past rainfall inputs, more rainfall is converted to event runoff. This relationship of runoff ratios with watershed saturation is also seasonal, with slightly higher runoff ratios in winter when there is more storage of water in the catchment due to decreased evapotranspiration losses. Event runoff ratios in Dead Run and Moores Run, both urban streams in Baltimore, ranged 0.38–0.88 and had a positive relationship with total event rainfall and antecedent moisture conditions However, event runoff ratios in Nine Mile Run are also not related to event precipitation inputs or antecedent moisture, suggesting that due to channel burial and rapid routing of runoff, there is minimal watershed storage of event water between events to affect the runoff ratio of the next event.

During the study period, 14 storm events had a runoff ratio greater than 1, meaning that there is more event water in the stream than precipitation inputs. We initially thought this was due to accumulated responses to multiple, closely-timed storms that confounded runoff accounting among events. Even after these events ($n = 6$) were eliminated, there are eight other events, all in the summer, with runoff ratios greater than 1. This 'water subsidy' could be from sewer overflows, hydrant flushes, or water line breaks. While the uncertainties in the stage-discharge relationship (Figure S1) can affect calculation of event runoff ratios, even with the lowest possible discharge from the stage-discharge relationship, there are still multiple events with runoff ratios exceeding 1. The phenomenon of urban water subsidies has been considered in other urban hydrology studies (Bhaskar & Welty, 2012; Kaushal & Belt, 2012; Pangle et al., 2022) and warrants further exploration, particularly because these subsidies are heterogenous in space and time. Pipe leakage is not evenly distributed around a watershed but concentrated in certain places (Bhaskar & Welty, 2012), and new fractures can form due to changes in weather, or old fractures can be repaired or blocked with debris and stop leaking (DeSilva et al., 2005), making attribution to one particular urban water source challenging. The likelihood of sewer overflows in Nine Mile Run is high due to proximity of sewage pipes—a large (1.4 m diameter) collector sewer pipe runs alongside the mainstream channel for its entire length—and advanced sewer age of this network (~100 years old) (Divers et al., 2013). While sanitary sewers are not designed to receive storm water, old pipes are subject to fractures, failures, and intrusion by tree roots that introduce opportunities for groundwater to infiltrate through pipe cracks and create flows that exceed pipe capacity. We have observed sanitary sewers overflowing through utility access points into the stream during many storm events. Inflow and infiltration of freshwater into sanitary sewers can constitute 20%–50% if the total flow (Bareš et al., 2012; Karpf & Krebs, 2011; Kracht et al., 2007; Kracht & Gujer, 2005; Pangle et al., 2022), and is the dominant cause of sanitary sewer overflows (EPA, 2004).

The remaining eight storms with runoff ratios greater than one fall into three groups based on the magnitude of the discharge peak: discharge peak less than 2 m^3/s, discharge peak 2–4 m^3/s, and discharge peak above 4 m^3/s. For the four storms below 2 m^3/s, we attribute the high runoff ratios (1.1–1.7) to water infrastructure failures such as drinking water main breaks and hydrant flushing. These storms all have low event precipitation (0.3–0.4 mm) that cannot account for the size of the discharge peaks (1.0–1.7 m^3/s), so the high runoff ratio could be due to the contribution of anthropogenic sources of water in the watershed. The two storms with discharge peaks of between 2 and 4 m^3/s also have low event precipitation (0.2 and 0.4 mm) but have high antecedent precipitation (6.5 and 15.7 mm), suggesting that higher soil saturation, and sewer pipes at higher capacity from previous storms may create favourable conditions for sanitary sewer overflows and lead to the observed event runoff ratios of 2.0 and 3.2, respectively. In the last case, the two storms with very high discharge peaks (17.7 and 24.4 m^3/s) have both high event precipitation and high antecedent precipitation, suggesting event precipitation filled pipes beyond capacity.

All storms with runoff ratios greater than one occurred in summer or the very end of spring, further supporting the role of high intensity convective thunderstorms for triggering sewer overflow events, especially when there are multiple consecutive high-intensity events in the watershed over several days. These overflow-driven streamflow subsidies are spatially heterogenous, and infrequent, but can still affect the hydrology, especially in a stream that is as responsive to storm drainage inputs as Nine Mile Run.

5 | CONCLUSIONS

While Nine Mile Run is comparable in size and imperviousness to many prominent urban watershed case studies (Konrad et al., 2005; Meierdiercks et al., 2010a; Smith et al., 2013; Smith, Miller, et al., 2005), it is considerably flashier by almost all metrics. We attribute this to the widespread (98%) stream burial of Nine Mile Run stream channels. The inconsistent linkage between flow events and antecedent precipitation, and the narrow range of runoff ratios observed throughout the year seem to result from the dominant piped drainage. Runoff ratios greater than one suggest considerable infrastructure failures and highlight the importance of urban water subsidies, such as sewer overflows and water main breaks, as important contributors to urban streams during storm events, especially those when systems are at capacity from previous storms.

We observed the largest and fastest event responses to convective summer thunderstorms, and it is these high intensity storms that are predicted to increase in frequency over the next several decades (Hirsch & Archfield, 2015). It is essential to support projects that build watershed retention capacity and mitigate the effects of urban flooding. However, this is no easy task. For example, while some studies show stormwater detention decreases peak flows (Pennino et al., 2016), other studies determined that the presence of stormwater management facilities have an negligible effect on reducing peak flows or discharge rise time (Miller et al., 2021). Our study results further underline limitations inherent in using stream restoration projects as end-of-pipe solutions to flashy urban streams. Hydrologic responses driven by buried headwaters can threaten the success of restoration projects when flows exceed design flows and wash out wetlands, riparian areas, and other habitat restoration interventions (Bain et al., 2014).

ACKNOWLEDGEMENTS

This material is based upon work supported by the National Science Foundation under Grant Nos. 1939977 and 1253000 to EM Elliott. This work was also supported by the Pittsburgh Water Collaboratory and the Mellon Pre-Doctoral Fellowship at the University of Pittsburgh. We would also like to thank Sarah Lavin for establishing the gage and developing early stage-discharge relationships, Joe Fedor for downloading stage data and sharing sewage pipe flow data and Krissy Hopkins for sharing her event selection code. We appreciate the comments and suggestions from Dr. Sarah Ledford and two anonymous reviewers for their improvement of the manuscript.

DATA AVAILABILITY STATEMENT

Radar precipitation data for Allegheny County can be downloaded from https://www.3riverswetweather.org/municipalities/calibrated-radar-rainfall-data. Nine Mile Run discharge data and analysis scripts can be made available upon request to ref61@pitt.edu.

ORCID

Rebecca Forgrave https://orcid.org/0000-0001-7240-6569

REFERENCES

3 Rivers 2nd Nature. (2006). Allegheny County: Landscape Ecology and Green Infrastructure. https://www.pasda.psu.edu/uci/DataSummary.aspx?dataset=1251

3 Rivers Wet Weather (2021). *Calibrated radar rainfall data*. https://www.3riverswetweather.org/municipalities/calibrated-radar-rainfall-data

Bain, D. J., Copeland, E. M., Divers, M. T., Hecht, M., Hopkins, K. G., Hynicka, J., Koryak, M., Kostalos, M., Brown, L., Elliott, E. M., Fedor, J., Gregorich, M., Porter, B., Smith, B., Tracey, C., & Zak, M. (2014). Characterizing a major urban stream restoration project: Nine mile run (Pittsburgh, Pennsylvania, USA). *Journal of the American Water Resources Association*, *15*, 218–1621. https://doi.org/10.1111/jawr.12225

Bareš, V., Stránský, D., & Sýkora, P. (2012). Evaluation of sewer infiltration/inflow using COD mass flux method: Case study in Prague. *Water Science and Technology*, *66*(3), 673–680. https://doi.org/10.2166/wst.2012.229

Bhaskar, A. S., & Welty, C. (2012). Water balances along an urban-to-rural gradient of metropolitan Baltimore, 2001–2009. *Environmental and Engineering Geoscience*, *18*(1), 37–50. https://doi.org/10.2113/gseegeosci.18.1.37

Blume, T., Zehe, E., & Bronstert, A. (2007). Rainfall-runoff response, event-based runoff coefficients and hydrograph separation. *Hydrological Sciences Journal*, *52*(5), 843–862. https://doi.org/10.1623/hysj.52.5.843

Bonneau, J., Fletcher, T. D., Costelloe, J. F., & Burns, M. J. (2017). Stormwater infiltration and the 'urban karst' – A review. *Journal of Hydrology*, *552*, 141–150. https://doi.org/10.1016/j.jhydrol.2017.06.043

Bornstein, R., & Lin, Q. (2000). Urban heat islands and summertime convective thunderstorms in Atlanta: Three case studies. *Atmospheric Environment*, *34*(3), 507–516. https://doi.org/10.1016/S1352-2310(99)00374-X

Broadhead, A. T., Horn, R., & Lerner, D. N. (2013). Captured streams and springs in combined sewers: A review of the evidence, consequences and opportunities. *Water Research*, *47*(13), 4752–4766. https://doi.org/10.1016/j.watres.2013.05.020

Buda, A. R., & DeWalle, D. R. (2009). Dynamics of stream nitrate sources and flow pathways during stormflows on urban, forest and agricultural watersheds in Central Pennsylvania, USA. *Hydrological Processes*, *23*(23), 3292–3305. https://doi.org/10.1002/hyp.7423

DeSilva, D., Burn, S., Tjandraatmadja, G., Moglia, M., Davis, P., Wolf, L., Held, I., Vollertsen, J., Williams, W., & Hafskjold, L. (2005). Sustainable management of leakage from wastewater pipelines. *Water Science and Technology*, *52*(12), 189–198. https://doi.org/10.2166/wst.2005.0459

Dingman, S. L. (2002). *Physical hydrology* (p. 646). Prentice Hall.

Divers, M. T., Elliott, E. M., & Bain, D. J. (2013). Constraining nitrogen inputs to urban streams from leaking sewers using inverse modeling: Implications for dissolved inorganic nitrogen (DIN) retention in urban environments. *Environmental Science and Technology*, *47*(4), 1816–1823. https://doi.org/10.1021/es304331m

Drum, R. G., Noel, J., Kovatch, J., Yeghiazarian, L., Stone, H., Stark, J., Kirshen, P., Best, E., Emery, E., Trimboli, J., Arnold, J., & Raff, D. (2017). *Ohio River Basin: Formulating climate change mitigation/adaptation strategies through regional collaboration with the ORB alliance*. Civil works technical report, CWTS 2017-01. Alexandria, VA: U.S. Army Corps of Engineers, Institute for Water Resources (Issue May). http://www.lrh.usace.army.mil/Portals/38/docs/orba/USACE%20Ohio%20River%20Basin%20CC%20Report_MAY%202017.pdf

Duncan, H. P. (2019). Baseflow separation – A practical approach. *Journal of Hydrology*, *575*, 308–313. https://doi.org/10.1016/j.jhydrol.2019.05.040

Elmore, A. J., & Kaushal, S. S. (2008). Disappearing headwaters: Patterns of stream burial due to urbanization. *Frontiers in Ecology and the Environment*, *6*(6), 308–312. https://doi.org/10.1890/070101

EPA (2004). *Report to congress on impacts and control of combined sewer overflows and sanitary sewer overflows*. https://www.epa.gov/npdes/2004-npdes-cso-report-congress

Fuka, D., Walter, M., Archibald, J., Steenhuis, T., & Easton, Z. (2018). *EcoHydRology, R Package*. CRAN. https://cran.r-project.org/web/packages/EcoHydRology/EcoHydRology.pdf

Georgakakos, A., Fleming, P., Dettinger, M., Peters-Lidard, C., Richmond, T., Reckhow, K., White, K., & Yates, D. (2014). NCA 2014: Chapter 3: Water resources. In *Climate change impacts in the United States: The third national climate assessment* (pp. 69–112). US Global Change Research Program. https://doi.org/10.7930/J0G44N6T

Graf, W. L. (1975). The impact of suburbanization on fluvial geomorphology. *Water Resources Research*, *11*(5), 690–692. https://doi.org/10.1029/WR011i005p00690

Haga, H., Matsumoto, Y., Matsutani, J., Fujita, M., Nishida, K., & Sakamoto, Y. (2005). Flow paths, rainfall properties, and antecedent soil moisture controlling lags to peak discharge in a granitic unchanneled catchment. *Water Resources Research*, *41*(12), 1–14. https://doi.org/10.1029/2005WR004236

Henderson, F. (1966). *Open channel flow*. Macmillan Publishing Co.

Hibbs, B. J., & Sharp, J. M. (2012). Hydrogeological impacts of urbanization. *Environmental and Engineering Geoscience*, *18*(1), 3–24. https://doi.org/10.2113/gseegeosci.18.1.3

Hirsch, R. M., & Archfield, S. A. (2015). Flood trends: Not higher but more often. *Nature Climate Change*, *5*(3), 198–199. https://doi.org/10.1038/nclimate2551

Historic Pittsburgh Maps (2021). *Pittsburgh historic maps*. University of Pittsburgh Library Digital Collections. https://www.arcgis.com/apps/View/index.html?appid=63f24d1466f24695bf9dfc5bf6828126

Hopkins, K. G., & Bain, D. J. (2018). Research note: Mapping spatial patterns in sewer age, material, and proximity to surface waterways to infer sewer leakage hotspots. *Landscape and Urban Planning*, *170*, 320–324. https://doi.org/10.1016/J.LANDURBPLAN.2017.04.011

Hopkins, K. G., Bain, D. J., & Copeland, E. M. (2013). Reconstruction of a century of landscape modification and hydrologic change in a small urban watershed in Pittsburgh, PA. *Landscape Ecology*, *29*(3), 413–424. https://doi.org/10.1007/s10980-013-9972-z

Hopkins, K. G., Bhaskar, A. S., Woznicki, S. A., & Fanelli, R. M. (2019). Changes in event-based streamflow magnitude and timing after suburban development with infiltration-based stormwater management. *Hydrological Processes*, *34*, 387–403. https://doi.org/10.1002/hyp.13593

Hopkins, K. G., Morse, N. B., Bain, D. J., Bettez, N. D., Grimm, N. B., Morse, J. L., Palta, M. M., Shuster, W. D., Bratt, A. R., & Suchy, A. K. (2015). Assessment of regional variation in streamflow responses to urbanization and the persistence of physiography. *Environmental Science and Technology*, *49*(5), 2724–2732. https://doi.org/10.1021/es505389y

Karpf, C., & Krebs, P. (2011). Quantification of groundwater infiltration and surface water inflows in urban sewer networks based on a multiple model approach. *Water Research*, *45*(10), 3129–3136. https://doi.org/10.1016/j.watres.2011.03.022

Kaushal, S. S., & Belt, K. T. (2012). The urban watershed continuum: Evolving spatial and temporal dimensions. *Urban Ecosystems*, *15*(2), 409–435. https://doi.org/10.1007/s11252-012-0226-7

Konrad, C. P., Booth, D. B., & Burges, S. J. (2005). Effects of urban development in the Puget lowland, Washington, on interannual streamflow patterns: Consequences for channel form and streambed disturbance. *Water Resources Research*, *41*(7), 1–15. https://doi.org/10.1029/2005WR004097

Kracht, O., Gresch, M., & Gujer, W. (2007). A stable isotope approach for the quantification of sewer infiltration. *Environmental Science and Technology*, *41*(16), 5839–5845. https://doi.org/10.1021/es062960c

Kracht, O., & Gujer, W. (2005). Quantification of infiltration into sewers based on time series of pollutant loads. *Water Science and Technology*, *52*(3), 209–218. https://doi.org/10.2166/wst.2005.0078

Kuliczkowska, E. (2017). Environmental and structural risk assessment of long operated vitrified clay sewers. *Environment Protection Engineering*, *44*(2), 53–67. https://doi.org/10.5277/epe170205

Kundzewicz, Z. W. (2008). Climate change impacts on the hydrological cycle. *Ecohydrology & Hydrobiology*, *8*(2–4), 195–203. https://doi.org/10.2478/V10104-009-0015-Y

Leopold, L. (1968). *Hydrology for urban land planning, A guidebook on the hydrologic effects of urban land use*. U.S. Department of the Interior.

Loehlein, M. D., Meeneghan, T. J., & Prevost, T. (2005). A continuous simulation approach for separate sewered areas. *Journal of Water Management Modeling*, *13*, 223–244. https://doi.org/10.14796/JWMM.R223-21

McMahon, G., Bales, J. D., Coles, J. F., Giddings, E. M. P., & Zappia, H. (2003). Use of stage data to characterize hydrologic conditions in an urbanizing environment. *Journal of the American Water Resources Association*, *39*(6), 1529–1546. https://doi.org/10.1111/j.1752-1688.2003.tb04437.x

Meierdiercks, K. L., Smith, J. A., Baeck, M. L., & Miller, A. J. (2010a). Heterogeneity of hydrologic response in urban watersheds. *Journal of the American Water Resources Association*, *46*(6), 1221–1237. https://doi.org/10.1111/j.1752-1688.2010.00487.x

Meierdiercks, K. L., Smith, J. A., Baeck, M. L., & Miller, A. J. (2010b). Analyses of urban drainage network structure and its impact on hydrologic response. *Journal of the American Water Resources Association*, *46*(5), 932–943. https://doi.org/10.1111/J.1752-1688.2010.00465.X

Merz, B., Vorogushyn, S., Uhlemann, S., Delgado, J., & Hundecha, Y. (2012). HESS Opinions: "More efforts and scientific rigour are needed to attribute trends in flood time series". *Hydrology and Earth System Sciences*, *16*(5), 1379–1387. https://doi.org/10.5194/hess-16-1379-2012

Miller, A. J., Welty, C., Duncan, J. M., Baeck, M. L., & Smith, J. A. (2021). Assessing urban rainfall-runoff response to stormwater management extent. *Hydrological Processes*, *35*(7), 1–11. https://doi.org/10.1002/hyp.14287

Napieralski, J., Keeling, R., Dziekan, M., Rhodes, C., Kelly, A., & Kobberstad, K. (2015). Urban stream deserts as a consequence of excess stream burial in urban watersheds. *Annals of the Association of American Geographers*, *105*(4), 649–664. https://doi.org/10.1080/00045608.2015.1050753

Napieralski, J. A., & Carvalhaes, T. (2016). Urban stream deserts: Mapping a legacy of urbanization in the United States. *Applied Geography*, *67*, 129–139. https://doi.org/10.1016/j.apgeog.2015.12.008

Napieralski, J. A., & Welsh, E. S. (2016). A century of stream burial in Michigan (USA) cities. *Journal of Maps*, *12*, 300–303. https://doi.org/10.1080/17445647.2016.1206040

Ntelekos, A. A., Smith, J. A., Baeck, M. L., Krajewski, W. F., Miller, A. J., & Goska, R. (2008). Extreme hydrometeorological events and the urban environment: Dissecting the 7 July 2004 thunderstorm over the Baltimore MD metropolitan region. *Water Resources Research*, *44*, 1–19. https://doi.org/10.1029/2007WR006346

Ogden, F. L., Raj Pradhan, N., Downer, C. W., & Zahner, J. A. (2011). Relative importance of impervious area, drainage density, width function, and subsurface storm drainage on flood runoff from an urbanized catchment. *Water Resources Research*, *47*(12), 1–12. https://doi.org/10.1029/2011WR010550

PAMAP Program Pennsylvania Department of Conservation and Natural Resources, Bureau of Topographic and Geologic Survey (2005). *PAMAP program – Land cover for Pennsylvania 2005*. http://www.pasda.psu.edu

Pangle, L. A., Diem, J. E., Milligan, R., Adams, E., & Murray, A. (2022). Contextualizing inflow and infiltration within the streamflow regime of urban watersheds. *Water Resources Research*, *58*, 1–19. https://doi.org/10.1029/2021wr030406

Pennino, M. J., McDonald, R. I., & Jaffe, P. R. (2016). Watershed-scale impacts of stormwater green infrastructure on hydrology, nutrient fluxes, and combined sewer overflows in the mid-Atlantic region. *Science of the Total Environment*, *565*, 1044–1053. https://doi.org/10.1016/j.scitotenv.2016.05.101

Poff, N. L. R., Allan, J. D., Bain, M. B., Karr, J. R., Prestegaard, K. L., Richter, B. D., Sparks, R. E., & Stromberg, J. C. (1997). The natural flow regime: A paradigm for river conservation and restoration. *BioScience*, *47*(11), 769–784. https://doi.org/10.2307/1313099

Roodsari, B. K., & Chandler, D. G. (2017). Distribution of surface imperviousness in small urban catchments predicts runoff peak flows and stream flashiness. *Hydrological Processes*, *31*(17), 2990–3002. https://doi.org/10.1002/hyp.11230

Roy, A. H., Dybas, A. L., Fritz, K. M., & Lubbers, H. R. (2015). Urbanization affects the extent and hydrologic permanence of headwater streams in a midwestern US metropolitan area. *Journal of the North American Benthological Society*, *28*(4), 911–928. https://doi.org/10.1899/08-178.1

Schreider, S. Y., Smith, D. I., & Jakeman, A. J. (2000). Climate change impacts on urban flooding. *Climatic Change*, *47*(1–2), 91–115. https://doi.org/10.1023/a:1005621523177

Schueler, T. R. (1994). The importance of imperviousness. *Watershed Protection Techniques*, *1*(3), 100–111.

Schueler, T. R., Fraley-Mcneal, L., & Cappiella, K. (2009). Is impervious cover still important? Review of recent research. *Journal of Hydrologic Engineering*, *14*(4), 309–315. https://doi.org/10.1061/ASCE1084-0699200914:4309

Sharp, J. M., Krothe, J. N., Mather, J., Garcia-Fresca, B., & Stewart, C. A. (2003). Effects of urbanization on groundwater systems. In *Earth science in the city: A reader* (pp. 257–278). American Geophysical Union.

Shuster, W. D., Bonta, J., Thurston, H., Warnemuende, E., & Smith, D. R. (2005). Impacts of impervious surface on watershed hydrology: A review. *Urban Water Journal*, *2*(4), 263–275. https://doi.org/10.1080/15730620500386529

Smith, B. K., Smith, J. A., Baeck, M. L., Villarini, G., & Wright, D. B. (2013). Spectrum of storm event hydrologic response in urban watersheds. *Water Resources Research*, *49*(5), 2649–2663. https://doi.org/10.1002/wrcr.20223

Smith, J. A., Baeck, M. L., Meierdiercks, K. L., Nelson, P. A., Miller, A. J., & Holland, E. J. (2005). Field studies of the storm event hydrologic response in an urbanizing watershed. *Water Resources Research*, *41*(10), 1–15. https://doi.org/10.1029/2004WR003712

Smith, J. A., Miller, A. J., Baeck, M. L., Nelson, P. A., Fisher, G. T., & Meierdiercks, K. L. (2005). Extraordinary flood response of a small urban watershed to short-duration. *Journal of Hydrometerology*, *6*, 599–617. https://doi.org/10.1175/JHM426.1

Soulsby, C., Birkel, C., & Tetzlaff, D. (2014). Assessing urbanization impacts on catchment travel times. *Geophysical Reserach Letters*, *41*, 442–448. https://doi.org/10.1002/2013GL058716

Trenberth, K. E. (1999). Conceptual framework for changes of extremes of the hydrological cycle with climate change. In T. R. Karl, N. Nicholls, & A. Ghazi (Eds.), *Weather and Climate Extremes* (pp. 327–339). Springer. https://doi.org/10.1007/978-94-015-9265-9_18

Valtanen, M., Sillanpää, N., & Setälä, H. (2014). Effects of land use intensity on stormwater runoff and its temporal occurrence in cold climates. *Hydrological Processes*, *28*(4), 2639–2650. https://doi.org/10.1002/hyp.9819

Walsh, C. J., Roy, A. H., Feminella, J. W., Cottingham, P. D., Groffman, P. M., & Morgan, R. P. (2005). The urban stream syndrome: Current knowledge and the search for a cure. *Journal of the North American Benthological Society*, *24*(3), 706–723. https://doi.org/10.1899/04-028.1

Weitzell, R., Kaushal, S., Lynch, L., Guinn, S., & Elmore, A. (2016). Extent of stream burial and relationships to watershed area, topography, and impervious surface area. *Water*, *8*(11), 538. https://doi.org/10.3390/w8110538

Wittenberg, H. (2003). Effects of season and man-made changes on baseflow and flow recession: Case studies. *Hydrological Processes*, *17*(11), 2113–2123. https://doi.org/10.1002/HYP.1324

Yang, L., Smith, J. A., Wright, D. B., Baeck, M. L., Villarini, G., Tian, F., & Hu, H. (2013). Urbanization and climate change: An examination of nonstationarities in urban flooding. *Journal of Hydrometeorology*, *14*(6), 1791–1809. https://doi.org/10.1175/JHM-D-12-095.1

SUPPORTING INFORMATION

Additional supporting information may be found in the online version of the article at the publisher's website.

How to cite this article: Forgrave, R., Elliott, E. M., & Bain, D. J. (2022). Event scale hydrograph responses highlight impacts of widespread stream burial and urban infrastructure failures. *Hydrological Processes*, *36*(5), e14584. https://doi.org/10.1002/hyp.14584